Development of Test Method for Evaluating Filtration Performance of A Filter Element

by

Suzanna Juyanty Binti Mohd Jeffry

Dissertation submitted in partial fulfillment of
the requirements for the
Bachelor of Engineering (Hons)
(Chemical Engineering)

JANUARY 2005

Universiti Teknologi PETRONAS
Bandar Seri Iskandar
31750 Tronoh
Perak Darul Ridzuan

CERTIFICATION OF APPROVAL

Development of Test Method for Evaluating Filtration Performance of A Filter Element

by

Suzanna Juyanty Binti Mohd Jeffry

A project dissertation submitted to the
Chemical Engineering Programme
Universiti Teknologi PETRONAS
in partial fulfillment of the requirement for the
BACHELOR OF ENGINEERING (Hons)
(CHEMICAL ENGINEERING)

Approved by,

(Mrs. Noorfidza Binti Yub Harun)

UNIVERSITI TEKNOLOGI PETRONAS
TRONOH, PERAK
January 2005

CERTIFICATION OF ORIGINALITY

This is to certify that I am responsible for the submitted in this project, that the original work is my own except as specified in the references and acknowledgements, and that the original work contained herein have not been undertaken or done by unspecified sources or persons.

SUZANNA JUYANTY BINTI MOHD JEFFRY

ACKNOWLEDGEMENT

First and foremost, the author would like to thank the Almighty for all His blessings that made all things possible in this project.

The author would also like to take this opportunity to thank all parties involved in making the Chemical Engineering Final Year Research Project, ECB 5034 a success. Greatest compliments also go to Universiti Teknologi PETRONAS's Final Year Research Project Committee for giving the author the chance to explore her intellectual capabilities by participating in the research project. The author would also like to express warmest gratitude and appreciation to Pn. Noorfidza Binti Yub Harun and Prof. Dr. V. R. Radhakrishnan, for tireless and endless efforts by providing guidance and assistance throughout this challenging experience.

The author's deepest appreciation also goes to Malaysian Air Filter R&D Engineer, Mr Faizal B. Mohd Mujer for all the support and patience in throughout the project completion.

Heartfelt appreciation also goes to lecturers and UTP staffs for providing additional support and advice throughout the research project. The author's gratitudes also go to Mr. Zaaba Mohammad, Mr. Mahathir Mohammad and other technicians for their time, support and expertise.

Also, compliments to all personnel who have directly and indirectly contributed towards the success of this project. The efforts and commitments are truly valued and appreciated.

The author

ABSTRACT

Filtration process has wide range of applications in the industry, commerce and domestic life. It has been rightly said that the heart of any filter is the *filter medium*. Hence, it is important that filter medium has the combination of properties to ensure the effectiveness of filtration process. Two crucial methods to predict efficiency of a filter medium are by addressing its *porosity (the ratio of void volume to bulk volume)* and *permeability (the ease of otherwise with which that fluid flows through the medium).*

Currently, filters produced by a local company are sent to overseas for performance testing. However, due to cost and equipments availability, it is proposed to develop the test procedure locally. The project's objectives are mainly to study the characteristics and develop physical and quantitative test methods for the porosity and permeability measurements of fibrous filter media rated 10, 28 and 50 micron supplied by the local company.

Two methods are applied to evaluate the samples in this project. First method is by imaging using Scanning Electron Microscope (SEM). From the images, observation is done to evaluate the samples' structures and porosity calculations are done using ArcView GIS 3.2 Software. The second part is by performing gas flow test to calculate permeability, average permeability coefficient, flow average pore diameter, fiber diameter, specific pore diameter and viscous-term coefficient. Then, these values are compared with the filter media sizes.

From the study, it can be concluded that

- Fibrous filter media internals are consists of large number of fiber layers, each sparsely populated and distributed throughout the length, width and thickness.
- Porosity values are independent of the filter sizes for fibrous filter media as the pores in fibrous filter media are randomly oriented.
- Permeability values increase as filter media sizes increases which show that the ease for fluid flow increases as the sizes of open pores increases.

List of Figures **Page**

List of Tables **Page**

List of Abbreviations

A	Area of the filter medium [m^2]
d	Diameter [m]
d	Specific diameter [m]
$\boldsymbol{d}$	Flow average pore diameter [m]
d_f	Fiber diameter [m]
d_p	Particle diameter in a fluid passing through a filter media [m]
g_c	Conversion constant [1kg.m/N.s^2]
k	Kozeny-Carman constant for fibers
K_p	inertia permeability coefficient [m]
K_v	permeability coefficient [m^2]
M	Molecular weight of the gas [kg/mole]
P	Average absolute pressures [Pa]
ΔP	Differential pressure [N/m^2]
Q	Volumetric flow rate of fluid [m^3/s]
R	Gas constant, 8314 [N.m/mole.T]
T	Absolute temperature, (^oC+273) [K]
u	velocity of fluid [m/s]
u^2	Downstream velocity [m/s]
V_o	Volume of void space in a filter medium [m^3]
V_s	Volume of solids [m^3]
z	Thickness of the medium [m]

Greek Symbols

α	Viscous-term coefficient [m^{-2}]
β	Inertia-term coefficient [m^{-1}]
ε	Porosity, in terms of ratio or percentage [%]
η	Absolute viscosity of the gas [N.s/m^2]
μ	Absolute viscosity of the gas [N.s/m^2]
τ	Tortousity factor = 1/ ε (ASTM F902)

TABLE OF CONTENTS

CHAPTER 1

INTRODUCTION

1.1 BACKGROUND OF STUDY

1.1.1 Filtration Technology

Filtration is both a process of major contemporary importance and one with its beginnings rooted in antiquity. Hardly a modern industry exists without some dependence on filtering operation. Large-scale filters are used in diverse processes treating millions of tons of chemicals, fluids and minerals. Also, the necessity of clean air exists along with the necessity for a large number of industrial processes; and certain parts of industry itself rely on clean air on exceptional quality. Many employees in industry or agriculture need to avoid exposure to airborne particulates and protection is usually provided by respirator filters or larger scale filtration units. The production of drinking water has been expanded by using reverse osmosis techniques. Small filters are found in every automobile, and exceedingly small ones ensure the reliable performance of sophisticated navigational and space-oriented equipment. In addition, others capture bacteria and traces of solid matter from gas and liquid streams so that delicate instruments can be assembled without defect, and beverages, medicine and food can be free form contaminant. It is clearly that, over the years, filtration has become a subject that draws on fluid mechanics, aerosol science, electrostatics and the science/engineering interface.

1.1.2 Filtration Process Definition

There are a number of definitions of the word "filtration" and "filter", which can vary considerably in comprehensiveness and clarity. The former reflects a process; meanwhile the latter describes the equipment on operating the process. Few explanations on filtration are as follows:

i) "Suspended solid particles in a fluid of liquid or gas are physically or mechanically removed by using a porous medium that retains the particles as a separate phase or cake and passes the clear filtrate" – *Christie John Geankoplis.*

ii) "Separation of a fluid-solids mixture involving passage of most of the fluid through a porous barrier which retains most of the solid particulates contained in the mixture" – *Robert H. Perry and Don W. Green.*

iii) "The process of separating dispersed particles from a dispersing fluid by means of porous media. The dispersing medium can be a gas (or gas mixture, most frequently air) or a liquid" – *Josef Pich, The J. Heyrovsky Institute of Physical Chemistry and Electrochemistry.*

By comparing all the definitions above, it is clear that filtration involves a process that separates the desired and undesired components of a fluid mixture by means of a porous medium that retains some of the particles and allows the rest to pass as filtrate/permeate. Also, it can be seen that the porous medium has an important role in defining filtration process, which shows that the porous medium acts as the source of the effectiveness and success of filtration.

There are two main purposes of filtration, which are

i) *To remove impurities from a fluid*
   Also called 'clarification' normally uses finely porous filter media, which intends to remove as much impurities as possible, and preferable all of it.

ii) *To recover valuable materials from suspension in a fluid (usually a liquid).*
   Also called 'harvesting', which aims for as complete recovery as possible of the wanted materials, but uses coarser media.

A *filter* is any *device in which separation is achieved among other components of a suspension or solution, in a fluid – which may be a liquid or a gas – where the separation is caused by mechanical means, without the involvement of a change in phase (Derek B. Purchas, et. al., 2002).* The bulk filtration processes involve the removal of particles, droplets or molecules from a fluid, by means of a physical barrier, the filter medium, through which they will not pass by virtue of their size.

By definition, *filter medium* is *any material that under the operating conditions of the filter, is permeable to one or more components of a mixture, solution or suspension, and is impermeable to the remaining components. (Derek B. Purchas, et. al., 2002).* The retained components may be particles of solid, droplets of liquid, colloidal material, or molecular of ionic species in solution, while the permeate (or filtrate) will normally be suspending fluid or solvent, possibly together with some of other components.

As one of the filtration-specific properties, porosity is important to characterize the flow resistance and also relate to other properties of the filter media. For example, both high porosity and fine pore size result from the use of finer particles, but at the expense of a decrease in mechanical strength. Also, a filter medium can be rated or categorized by addressing its porosity, in parallel with its materials of construction, thickness, viscous permeability (deduced from the ratio of fluid flow rate to driving pressure) and also whether porosity changes with depth.

This Final Year Research Project is mainly to study about the filtration characteristics of fibrous filter media with different micron ratings. As known, the successful performance of a filter station depends largely upon the filter media properties. The filter media samples are provided from the local company, which are made from resin impregnated paper are being used for high pressure gas streams, high pressure water injection and disposal and also for fluid processing.

Thus, there are two possible approaches to determine and evaluate the samples' characteristics in this project, which are by *surface distribution* using Scanning Electron Microscope (SEM) and also by *fluid-flow distribution* by applying Gas Flow Test. Then, the experimental results are to be compared to evaluate the methods.

1.2 PROBLEM STATEMENT

It is essential to evaluate commercial filter media manufactured for development of filter system designs and also improvements of filtration in the industry. In addition, there are various filter properties relate to filter performance. Hence, it is crucial for

filter manufacturers to evaluate their filter media before selling them to customers in order to know the marketability and most importantly the ability to withstand for their specific applications in the industry.

Currently, the filter media produced by a local company are sent to overseas for performance testing. However, due to cost and equipments availability, it is proposed to develop the test procedure locally. Thus, this research is a significant effort to determine the filter media porosity and permeability characteristics and also their related filter media properties for the development of air and water filtration technology.

1.3 OBJECTIVES AND SCOPE OF STUDY

The study is aimed to

i) Develop test method for porosity and permeability measurements in filter media.
ii) To relate the porosity and permeability values for filter media of different sizes
iii) Microscopically study the structure, characteristics and pore size distribution of resin impregnated paper filter media (fibrous filter media)

The development of the test methods for the filter media samples provided from the local company are consist of the following:

i) Physical Evaluation
   - Characterization of pores on filter media.
   - Fluid-flow test.

ii) Quantitative Evaluation
   - Microscopically counting and size evaluation of pores and porosity.
   - Calculation of permeability, flow average pore diameter and other relate parameters.

CHAPTER 2

LITERATURE REVIEW AND THEORY

2.1 FILTRATION AND FILTER MEDIUM CONCEPT

Being the 'heart' of a filter, the filter medium properties should fill the specific requirements of its applications in the industry. The basis of a 'mechanical filter' is that the filter medium or septum works as a porous screen, removing and retaining particles too large to pass through the openings which provide the porosity, but allowing the 'carrier' fluid to pass. Particles are collected on individual fibers by *numerous mechanisms.*

The most important of these are *direct interception, inertial impaction and diffusion. Direct interception* involves finite size of particles intercepted as it approaches the collecting surface to a distance equal to its radius. Sometimes called sieve-effect where the distance between fibers is smaller than the particle diameter, d_p. *Inertial impaction* results if a particle or droplet in the airstream fails to negotiate the tortuous path presented by the random fibers in the filter bed, collides with and adheres to a fiber. The intensity of this mechanism increases with increasing particle size and velocity of flow. *Diffusion* occurs when extremely small particles wander in 'Brownian motion' within the flow pattern of the airstream, enhancing the chances of colliding with each other and with fibers forming the filter medium. With decreasing particle size, the intensity of 'Browninan motion' and diffusion deposition increases [2].

Generally, filter media can be divided into two categories, which are *surface filter media* and *depth filter media.* Examples of surface filter media is sinter bond woven wire mesh, meanwhile depth filter media are cast membrane and fibrous material. For surface media, all pores rest on single plane and depends on direct interception

to trap particles, which allows contaminants smaller than the pore size to pass through as shown in Figure 1 [Pall Corporation].

Figure 1: Surface Filtration

For depth filter media, contaminants within the internal structure of the medium are captured. Pores are distributed throughout the thickness of the medium and alternate flow paths create tortuous passages and yield higher dirt holding capacity as shown in Figure 2 [Pall Corporation].

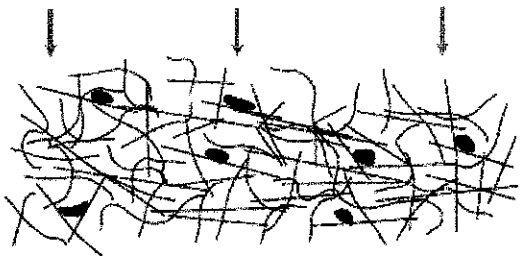

Figure 2: Depth Filtration

2.2 CLASSIFICATION, PROPERTIES AND CRITERIA OF CHOICE

A broad classification of media may be made on the basis of the basic mechanism involved in the separation of particles and fluids. Media that effect the separation by sieve-like action are perforated filters, edge filters plain-weave metal wire or monofilament cloths and certain grades of paper, where the particles are retained on the surface of the medium and pore penetration does not occur in a successful separation. Apart from particles that, by virtue of size, shape or adhesive properties, become lodged in the pores of such filters, particles are generally sieved out of lost as bleeds. These types of filter are generally for coarse suspensions. Second classification of filter media is for small particles that may be removed from flowing fluid by internal deposition. They are felts, mats, pads, multifilament yarn cloths and ceramics. Mechanisms such as internal sieving and electrostatic attachment to internal fibers occur for particle removal. Typical media types are shown in

Appendix 1 [2]. Practical filtration trials are used to test the suitability of filter media in meeting the following requirements [2]:

i) Efficient retention of particulate matter with clear filtrate
ii) Absence of medium binding of a sudden or progressive character
iii) Good cake discharge characteristics
iv) Adequate cleaning availability either by back-flushing or laundering
v) Physical strength and resistance to chemical attack
vi) Resistance to microorganisms

Purchas [3] also suggested that three criteria by which a filter medium to be judged:

i) What size of particle will be retained by the medium?
ii) What is the permeability of the clean medium?
iii) What is the solids-holding capacity of the medium and the resistance to fluid flow of the used medium?

Also, a successful filter medium is likely to be required to combine many different properties, ranging from its filtration characteristics and its chemical resistance to its mechanical strength, the dimensions in which it is available, and its wettability. These properties may be conveniently divided into three major categories as shown below and in detail in *Appendix 2* [1]:

i) *Machine-oriented properties*, which restrict the use of the medium to specific types of filter
ii) *Application-oriented properties*, which control the compatibility of the medium with the process environment
iii) *Filtration-specific properties*, which determine the ability of the medium to achieve a specified filtration task.

2.3 FIBROUS FILTER MEDIA

Fibrous filter media is one of the practical *depth type* filter media application. It comprises a layer, or mat, or numerous very fine fibers, of various diameter sizes ranging from 0.5 to 30 μm, depending on the material. These fibers are randomly oriented with each other, intermixed and intertwined so that they create a tortuous flow-passages or pores in which the particles are trapped and held by the

mechanisms stated previously in Section 3.1. Fibrous materials most commonly used are polymeric materials, cellulose, cotton, microglass fiber, and synthetics. *Appendix 3* gives the typical indication of the factors which influence the retention rates of depth filters. This shows that the void volume is important as one of the mechanical factors that affect the retention rate.

Relative efficiencies of these of filter media types are a function of fiber diameter, where narrower the fibers, the closer they can be compacted. The result is that smaller diameter fibers have smaller flow paths, therefore giving better filtration efficiency. Typically, the layer is 0.25-2 mm thick and is impregnated with resin (phenolic, epoxy or acrylate) to bind it together. The maintenance of a stable structure, including pore-size, and therefore of stable filtration characteristics throughout the medium's service life, referred to as the filter integrity, is a function of fiber-binding system. Fibrous filter media are used for the collection of sub-micrometer particles in clean air environments [4].

Papers are essentially sheets of fibrous non-woven materials made from organic fibers. In their basic form, they are essentially absorbent materials since they will 'swallow' up liquids and may well disintegrate under such action if the liquid is a solvent for the binder. Untreated paper elements used as filters, therefore, have very low mechanical strength and so their application as mechanical filters is strictly limited. By nature, papers have random fiber structure, although this can be controlled to a large extent in manufacture, and relatively low permeability. Due to the tortuous nature of the through-path, only relatively thin sheets can be used for practical filtering and even then the specific resistance is high. However, treated papers have two great advantages as filter media, which are:

i) They can be given a nominal cut-off of 10-20 μm or better, with a capability of removing a high proportion of much finer particles
ii) They are quite inexpensive materials as shown in *Appendix 4*

However, their chief disadvantages are:

i) High specific resistance
ii) Limited mechanical strength

To offset the former, paper filter elements are commonly used in *pleated form*, considerably increasing the superficial area for a given size of element. This

substantially reduces the flow velocity through the paper, and hence the effective or overall resistance to flow. Pleating also improves the rigidity of the element, although it is normally fully supported by a perforated inner tube. Depth of pleating is usually in the order of one quarter the diameter of the element [4].

Variations on the simple pleated form include corrugating as well as pleating that paper, which has the effect of increasing both the surface area and to some extent the stiffness, or dimpling of the surface or attachment of separator strips to maintain constant spacing and prevent the collapse of the pleats. Collapse of a pleated element will reduce the effective surface area, if excessive, may lead to tearing. The mechanical strength limitations of paper elements normally set at maximum working pressure for such types at about 7 bar. This can be improved by rigid reinforcement, for example a wire mesh backing, but higher pressures also increase the chance of element migration. This is always a possibility with paper elements, especially if they become choked and the system does not incorporate a pressure relief valve to bypass the element [4].

An inherent limitation with paper elements is that the very nature of the material does not provide an absolute cut-off figure. There will almost certainly always be larger pore sizes than the nominal rating and so random larger particles may be passed by the filter. This limits the suitability of paper elements for ultra-fine filtering. On the other hand, the performance of paper and particularly resin-impregnated paper elements can be superior to felts, fabrics, cotton cloths and similar media. Although paper filter elements are invariably thin, the tortuous path provided by the layer of fibers does mean that they filter in depth instead of acting as simple mechanical screens. At the same time, contaminants will collect mainly on the surface and the accumulation of such contaminants will progressively increase the efficiency of the filter by acting as a filter bed. Some solid contaminants will tend to penetrate into depth of paper and become lodged can make cleaning difficult or even impractical. However, some paper elements are reusable for 'dry' fluid cases, such as air. With 'wet' fluids, it is more usual to employ disposable filter elements, which are simply replaced when clogged [4].

Papers are also used to a limited extent for filter cloths in filter presses. A paper cloth air filter, for example, is basically a single-cell filter press, although more elaborate forms of element are normally used in panel filters. Papers are also used to face filter cloths.

2.4 PORE SIZE, POROSITY AND PERMEABILITY OF FILTER MEDIA

2.4.1 Pore Size and Porosity of Filter Media

A *pore* is a small channel or opening in a filter media, which allows passage of fluid.

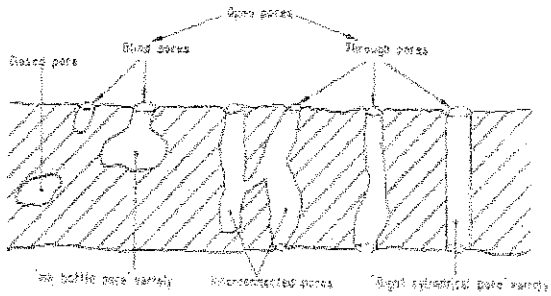

Figure 3: Schematic Representation of Types of Pores

Filter media are manufactured with various pore designs to meet its applications. The design can be divided into two, which are [Pall Corporation]:

- *Fixed or non-fixed*
    - *Fixed* – pore sizes do not change during the service life of the filter media
    - *Non-fixed* – pore sizes change during service life, e.g. pore enlarges due to pressure build-up, which subjected to unloading, channeling and media migration

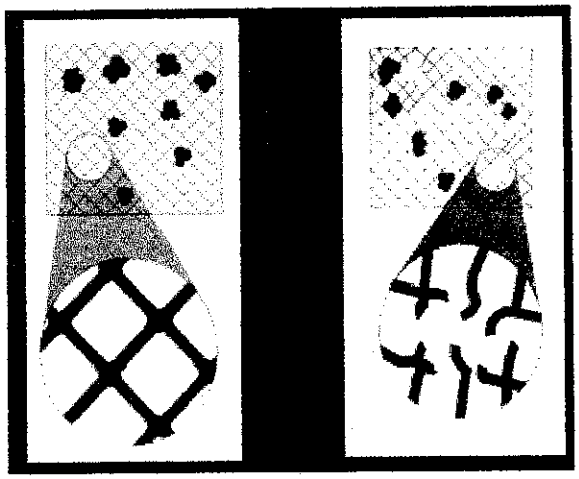

Figure 4: Fixed and Non-Fixed Pore

- *Uniform or non-uniform*
  - *Uniform* – all pores are of the same sizes and particles are captured by bridging
  - *Non-uniform* – the pores are distributed to different sizes

It is also noticed that not all pores are of the same size, especially for fibrous filter media. Indeed, there is relatively broad distribution of pore sizes in a given area. Hence, it is important in this study to consider the meaning of *average pore size.* When considering how a fluid flow through the media defines different paths, or tunnels, it can be realized that within each tunnel, the diameter varies along the length and different tunnels have different lengths. Thus, to deduce the average pore size needs for considering average of many distributions.

There are three distribution types can be addressed in considering a pore size distribution and the corresponding *average pore size* [5]:

i) *Number distribution:* By considering a list of the counts of pores of different diameters. Such distribution is measured by examining the face of the filter medium.

ii) *Volume distribution:* The cross-sectional opening is said to have 'unit' depth, in that the volume of a pore is proportional to the square of the diameter, d^2. The volume distribution is measured using mercury-intrusion test or liquid-drainage test.

iii) *Fluid flow distribution:* When a fluid in viscous flow, under a given driving force, confronts a pore, the volumetric flow rate of that fluid through the pore is proportional to the square of the cross-sectional area, d^4.

Thus, the *flow average* pore diameter is larger than the *volume-average*, which in turn, is larger than the *number-average*. Yet, some writers say that the volume-distribution of pore diameters is the same as the fluid-flow distribution.

Although it has been suggested that it is doubtful whether information on the pore size of a medium will be of much use in finalizing media selection, there is obviously great value in having such information since, in the limit, the pore structure of the medium will determine the feasibility of separation. The pore size of a medium, particularly for filters of the edge, perforated, simple wire, or monofilament type, is of use in deciding the upper limit of aperture size required by a particular process. For filters composed of random fibers, sintered or porous elements, staple or natural fiber cloths, the mean pore size will have less significance and use in predicting media behavior [2]. However, it is convenient to know the average value of the pore size to know the mean size of the open spaces in the fibrous filter media.

Porosity can be described as *the ratio of pore volume to total volume of a filter media expressed as percent.* Described in three-dimensional sense, if 10% of the bulk volume of the filter media is void space, the *porosity,* ε would be 0.10. With some types of media, direct measurement is possible of the relative areas of free and obstructed surface.

For fibrous materials, such as cellulose paper and filter sheets, the porosity range is up to 90% [1]. Also, *refer to Appendix 5* for typical filter media porosity values. Control of porosity in terms of pore volume, size and their distribution is important in hundreds of industries, products and processes.

2.4.2 Permeability of Filter Media

Another important term, *permeability,* is a vital measure of the medium's capability for filtration, is determined experimentally, generally by observing the rate of flow of a fluid under a defined pressure differential. *Permeability* of a porous medium is defined as *a measure of the ease with which a fluid will flow through its voids.* The immense variety of expressions formerly used for the permeability of filter media is shown in *Appendix 6* that was originally assembled in 1966. Air and water are the most common fluids most widely used in the assessment of permeability, although in certain fields other liquids such as oils are used. The most common form for expressing permeability disregards the thickness of the medium, so that the permeability is empirically quantified by the flow rate of air per unit area, under a defined differential pressure [1].

An appropriate example of this method is the Frazier scale widely used internationally in the paper and textile industries. During the test, an upstream air of gauge 0.5 lb_f/square inch (psi) is applied to a two-inch diameter disk filter medium with the downstream face is exposed to the atmosphere (zero gauge pressure). The air flow from the downstream face is reported as $ft^3/min.ft^2$.

Hence, as pointed out above, the permeability of a clean filter medium has a direct influence on the pressure losses occurring during filtration and also on the fluid flow conditions during the build-up of the first layers of the filter cake. In other words, the permeability of clean media predetermines power requirements and the initial flow rate of fluid through the filter. It has been observed that the initial flow rates can influence the structure of filter cake, resulting in changes in specific resistance of the deposit [2].

A fundamental expression for permeability coefficients of a medium are defined by Darcy Equation, which describes the flow through a porous layer,

$$\Delta P = \frac{Q\mu z}{K_v A} + \frac{\rho Q^2 z}{K_I A^2} \qquad (1)$$

Where:

K_v = permeability coefficient, m^2

K_p = inertia permeability coefficient, m

u = velocity of fluid, m/s

μ = absolute viscosity of the gas, $N.s/m^2$

z = thickness of the medium, m

ΔP = differential pressure across the filter media, N/m^2

Q = volumetric flow rate of fluid, m^3/s

A = area of the filter medium, m^2

For low flow rates or high viscosities (viscous flow), the second, inertial term in the Equation (1) becomes negligible and the equation becomes:

$$\Delta P = \frac{Q\mu z}{K_v A} \tag{2}$$

Hence, rearranging Equation (2) results to

$$K_v = \frac{1}{\alpha} = \frac{u\mu z}{\Delta P} = \frac{Q\mu z}{A\Delta P} \tag{3}$$

Where:

α = viscous-term coefficient, m^{-2}

By common empirical quantification of permeability, which is the flow rate of air per unit area, under a defined differential pressure and further rearrangement of Equation (3), the permeability value can be deduced by

$$\frac{Q}{A\Delta P} = \frac{K_v}{\mu z} \text{ in the units of } \frac{m^3/s}{m^2 Pa} \tag{4}$$

2.4.3 Porosity and Permeability Relationship

The *resistance to flow of a filter medium* depends both upon *the size of the individual pores and on the number of pores per unit area.* This resistance can be of major importance in industrial applications, since it may affect both capital and running costs, so that considerable care may be required in selecting a medium for a specific duty. The *actual resistance to flow of a fluid through a clean medium* is a

combination of the porosity of the medium material and also the permeability of the medium to the appropriate fluid [1].

The magnitude of permeability is determined by the degree of 'openess' of the medium, which would be more formally interpreted by the porosity of the medium and the sizes of pores present in its internal structure. The simplest and probably most widely used, model to relate permeability coefficient to the porosity of a filter medium through combining the concepts of porous media is introduced by Kozeny (1927) and Carman (1938). An example for this relationship, which can be applied for fibrous filter media [5]:

$$K_v = \frac{\mathbf{d}^2\varepsilon}{32\tau} = \frac{\mathbf{d}^2\varepsilon^2}{32} = \frac{d^2\varepsilon}{16k} \qquad (5)$$

Where:

d = flow average pore diameter, m

τ = tortousity factor = 1/ ε (ASTM F902)

The derivation for this relationship (Johnston 1992c) is shown in *Appendix 7*

d = specific diameter, m

ε = porosity in ratio

k = Kozeny-Carman constant for fibers (see Figure 5)

ε	0.2	0.3	0.4	0.5	0.6	0.7	0.8	0.9
k	2.7	3.8	4.9	5.8	6.3	6.6	7.2	9.8

Figure 5: Values of *k* for a Random Array of Fibers

Also, the fiber diameter can also be determined from the relationship:

$$d = \frac{d_f\varepsilon}{1-\varepsilon} \qquad (6)$$

Where:

d_f = fiber diameter, m

2.5 FILTRATION PROPERTIES TEST METHODS

There is a wide range of test methods to evaluate filter medium properties that have been developed according to various standards available today. These test method purposes are different from one another to yield various results.

Some major test methods for permeability testing in the industry are (*refer to Appendix 8*) [1]:

i) *Frazier Test*: Measuring permeability (as described earlier in Section 3.3.2)
ii) *Coulter Porometer*: Permeability measurement by pore analyzing
iii) *Gurley Densometer*: Air permeability measurement in paper industry
iv) *SDL Electronic Air Permeability Tester*: Developed by Shirley Institute for all kinds of flat materials.

Major test methods for porosity measurement are (*refer to Appendix 9*) [1]:

i) *Bubble Point Testing*: Utilizes a controlled air pressure to empty through pores that had previously been filled with a wetting liquid. A simple relationship between pressure, the properties of the liquid and the diameter of an identical circular pore permits calculation of the equivalent pore diameter. Suitable for pore sizes range 0.05μm-50μm.
ii) *Challenge Tests*: Determine the effective size of open pores by challenging with suspensions of particles of known sizes. Suitable for pore sizes range 0.005μm-100μm.
iii) *Mercury Porosimetry*: Involves filling the pores with mercury under pressures up to 400 MPa. The volume of mercury forced in is related to pore size and pressure by the same relationship used in the bubble point test. Suitable for pore sizes range 0.003μm-400μm.
iv) *Gas Adsorption*: Measuring the quantity of nitrogen adsorbed as its relative pressure is progressively increased at a constant cryogenic temperature. For pore sizes range 0.0004μm-0.04μm.

In this project, two methods are being applied to evaluate the filter samples' structure, porosity and permeability, which are by Scanning Electron Microscope (SEM) and Gas Flow Test.

2.5.1 Scanning Electron Microscope (SEM)

Number distribution is one of the methods of considering filters with wide range of pore sizes. By examining the face of the filter medium, the estimated porosity can be obtained by counting 2-dimensionally.

This method is also done based on the important theory stated by Abbot, 1963, in his book, *Flatland.* To extend the *Flatland* (2-dimensional) pore size distribution view to a three-dimensional view, consider that a fibrous filter medium is composed of many theoretical, thin layers. *The pore size distribution in one layer is the same as the next layer; however, a large pore in one layer does not necessarily lie in the same spot on the next layer.* Thus, *once a fluid penetrates the first layer, an individual stream, on meeting the next layer, may either divide into smaller streams or combine with adjacent streams to make a larger streams and cycle is repeated as the fluid goes on to the next layer across the thickness of the filter medium.* Hence, by using SEM, the surface topography of the filter media may be studied. The surface distribution is assumed to be the same as volume distribution using the assumption stated above.

2.5.2 Gas Flow Test

Most of test procedures are designed to characterize a medium in respect of the filtration-specific properties, which involves 'challenging' the medium. *Challenging with a clean fluid permits evaluation of:*

- The *permeability or resistance to flow per unit area of medium,* such as the flow rate of air or water under a defined pressure
- The *size of pores of the medium,* in terms of the ideal cylindrical pores assumed in the bubble point test, and hence an approximation of the size of particle that the medium can retain by straining mechanisms

The lab-scale gas-flow test applied in the project is similar to the Frazier test. As the rating of the filter media samples are 10 micron, 28 micron and 50 micron, the test can be applied using its specific equations for the rated pore diameter larger than 1.0 micron.

Theoretically, to perform the gas-flow test, the filter media is placed in between a pipeline. Air is flowed through the filter media, while the upstream flow rate is recorded. The pressure of both upstream and downstream are also noted. With increasing pressures on the upstream face, the corresponding increases in gas flow are recorded. It is crucial to ensure that the pressure-drop measurements across the media do not include the pressure drop across the housing.

From the test, a plot of downstream velocity, u^2 (or downstream volumetric flow rate) versus the product of the pressure differential and the average absolute pressures, $\Delta P \bullet \mathbf{P}$ is to be done. For filter media rated as having pores larger than 1 micron, the plot will look like Line 1 in Figure 6. The line starts out with a slope of 1.0, in viscous flow and then falls to 0.5 in inertia flow.

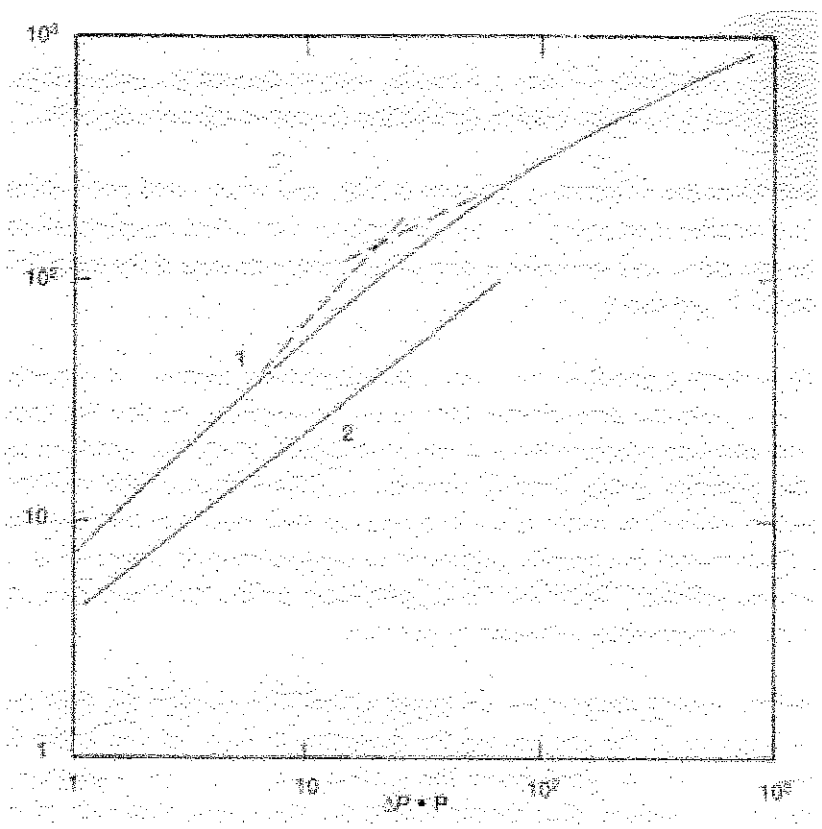

Figure 6: Example of gas-permeability measurement on filter media. The units are arbitrary, but show log/log plots of the velocity of the gas, u_2, leaving the downstream face of the filter medium, as a function of the product of the differential pressure, ΔP, and the average of the absolute pressures on both faces, P. Line 1 is seen with ordinary media; i.e., the slope starts out as 1.0, in viscous flow, and falls to 0.5, in inertia flow. Line 2 is

seen with small pore media; it remains straight, but with a slope between 1.0 and 0.5, showing a combination of viscous and slip flow; apparently inertia flow is never reached.

In those filter media, the description of gas flow is made as follows:

$$\frac{\Delta P\mathbf{P}}{z} = \alpha\eta P_2 u_2 + \frac{\beta(P_2 u_2)^2 M}{R g_c T} \qquad (7)$$

Where:

ΔP = P1-P2 = differential pressure across the filter media, N/m^2

P = average absolute pressure, $(P_1+P_2/2)$

z = thickness of the medium, m

α = the viscous-term coefficient, m^{-2}

η = absolute viscosity of the gas, $N.s/m^2$

β = the inertia-term coefficient, m^{-1}

u_2 = velocity of gas leaving the downstream face, m/s

M = molecular weight of the gas, kg/mole

R = gas constant, 8314 N.m/mole.T

T = absolute temperature, K (°C+273)

g_c = conversion constant, $1 kg.m/N.s^2$

By applying Equation (5), the flow-average pore diameter, **d**, can be deduced from:

$$\mathbf{d}^2 = \frac{32 u_2 \eta z P_2}{\varepsilon^2 \Delta P\mathbf{P}} \qquad (9)$$

And

$$\varepsilon = \frac{V_o}{(V_o + V_s)} \qquad (10)$$

Where:

V_o = volume of void space in a filter medium

V_s = volume of solids

CHAPTER 3

METHODOLOGY/PROJECT WORK

3.1 PROJECT FLOW DIAGRAM

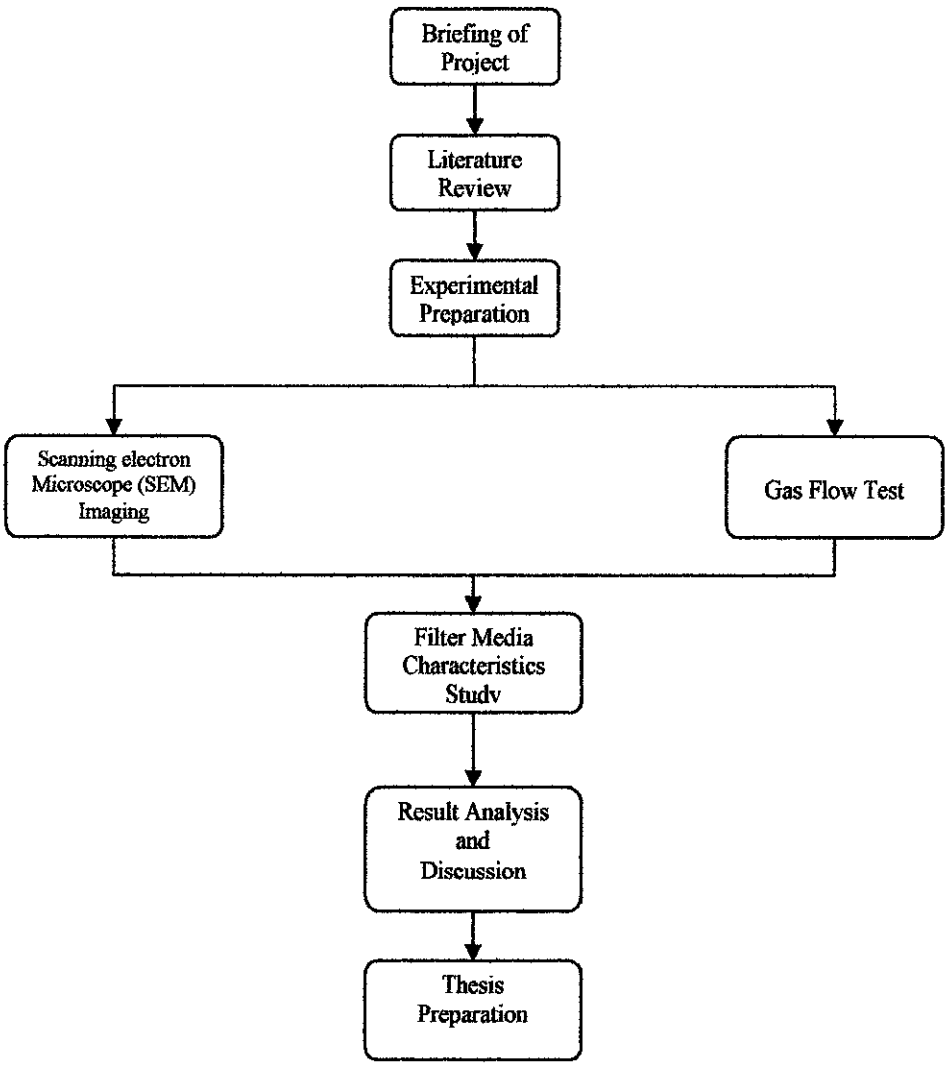

Figure 7: Project Methodology

3.2 PROCEDURE IDENTIFICATION

In order to achieve the objectives of this research project, the two methods shown above, which are SEM imaging and laboratory scale gas flow test are developed based on theoretical explanation of *number distribution and fluid flow distribution* characteristics of the filter media pores [5].

All the three filter media samples under test are examined using both the methods in order to compare and observe the effect of different filter media sizes on its characteristics. The description of the samples is as follows:

Type:	Resin impregnated paper
Sizes/Rating:	10, 28 and 50 micron
Homogenity:	Non-homogeneous (*refer to Appendix 10*)
Conductivity:	Non-conductive
Other Properties:	*Refer to Appendix 10*

3.3 TOOLS REQUIRED

3.3.1 Scanning Electron Microscope (SEM)

It is an excellent tool for analyzing the surface topography of a specimen three dimensionally. With the ability for variable pressure operation, magnification range 15X to 300kX, 5 axis motorised high precision geared stage in extra large chamber, extensive annotation and measurement facilities, 3072 x 2304 pixel image store with square pixels and 3 built in 'real time' image processing modes, SEM suitable when enhanced depth of field imaging is required. The schematic diagram of an SEM is shown in Figure 9.

Figure 8: Scanning Electron Microscope Model LEO 1430VP

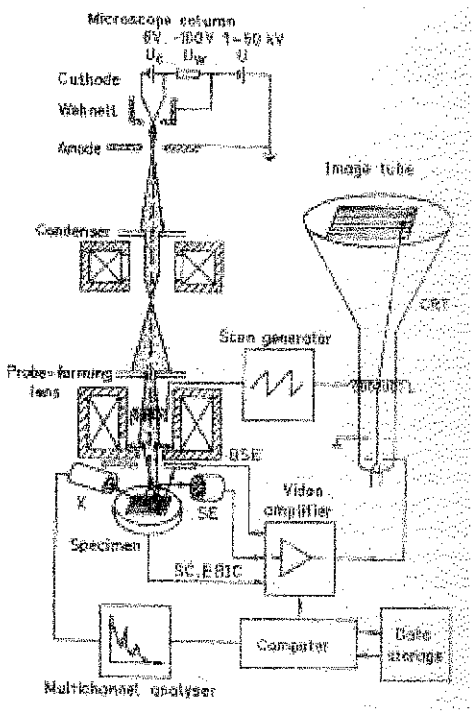

Figure 9: Principle of Scanning Electron Microscope (SEM) Showing a Two-Stage Demagnification of the Electron Source and The Detection of Secondary electrons (SE), Backscattered Electrons (BSE), Specimen Current (SC), Electron-Beam-Induced Current (EBIC) on A Cathode Ray Tube (CRT) and X-Ray Microanalysis.

Using Scanning Electron Microscope (SEM) Model LEO 1430VP, electrically conductive materials may be examined directly meanwhile non-conductive materials

may require a thin conductive (e.g. platinum is used for this experiment) coating to prevent electrical charging of the specimen. Sample sizes are limited to 10 cm in diameter. An electron beam passing an evacuated column is focused by electromagnetic lenses onto the specimen surface. The beam is then rastered over the specimen in synchrony with the beam of a cathode ray display screen. The secondary electron (inelastically scattered) emission from the sample (determined to a large extent by the surface topography) is then used to modulate the brightness of the cathode ray display screen, thereby forming the image. Should (elastically) back scattered electrons be used to form the image, the image contrast is determined largely by compositional differences of the sample surface rather than topographic features.

There are two main procedures for this experiment, which are:

1. *Sample Imaging:*

   The samples are cut in dimensions of 1 cm x 0.8 cm for testing. After starting-up and inspection on equipment, the sample chamber is vented. Then, the sample under test is loaded into the chamber and the sample is pumped down to vacuum. After switching on the electron gun and varying the EHT (Extra High Tension or beam voltage) at desired value, the sample is ready for viewing. In order to obtain a clear image, the brightness is maximized, the contrast is adjusted, the magnification is decreased and the image is focused until the image can be seen (*refer to Appendix 11* for detail procedures on sample imaging). Then, the region of interest is chosen and the right magnification is adjusted for the desired quality of image. Each sample is tested three times to obtain more accurate results.

2. *Sample Analyzing:*

   For analyzing fiber structure, the SEM images are directly examined and observed to see the internal arrangement and characteristics of the individual fibers. Meanwhile, for porosity calculation, the images are analyzed using **ArcView GIS 3.2 Software**. It is full-featured software for visualizing, managing, creating, and analyzing geographic data. Hence, the software helps user to understand the geographic context of specified data, allowing user to see relationships and identify patterns in new ways and solves problems faster. As the fiber patterns are random, the software provides help

to evaluate and integrate data/image easily. The images acquired from SEM, which are in the ".tiff" image extensions, are directly analyzed using the software. The software provides precise tool to calculate areas of various shapes on the images. Hence, by highlighting the appropriate area to be known, the area can be obtained directly. In order to calculate the porosity of the sample images, the total area of the image is calculated first. The total area for all the open spaces on the images is then calculated. Hence, the porosity value can be obtained by dividing the former value with the latter.

3.3.2 Gas Flow Test

By using the theoretical definition of the gas flow test, the Cybron Asia Compressible Flow Bench is used to conduct the experiment. The equipment is selected as it is suitable in varying the air flow towards the pipeline by using the compressor. The equipment is consists of a compressor equipped with adjustable frequency panel and pipe clip to connect the downstream pipeline, a straight pipeline of 15 cm long and 3 cm diameter with a 0.5 cm orifice slot in the middle, and a digital hand-held manometer to record pressure drop values. Also, an analog anemometer is also used to record velocity and temperature values.

The samples are cut in diameters of 3 cm according to the pipeline dimension. The 15 cm long pipeline is connected to the compressor using the pipe clip. It is important to ensure that the connection is tightened so that there is no leakage across the line. The air at compressor suction, which is at atmospheric pressure and room temperature, is compressed to a certain temperature and pressure according to the compressor's frequency and power output. Then, the air is flowed through the pipeline and the filter medium under test before being released back to atmosphere as shown in Figure 10. The system is waited until stabilize. When, the values are constant, the reading for pressure drop across the filter medium and velocity of air at downstream of the filter medium are recorded using the digital manometer and the anemometer.

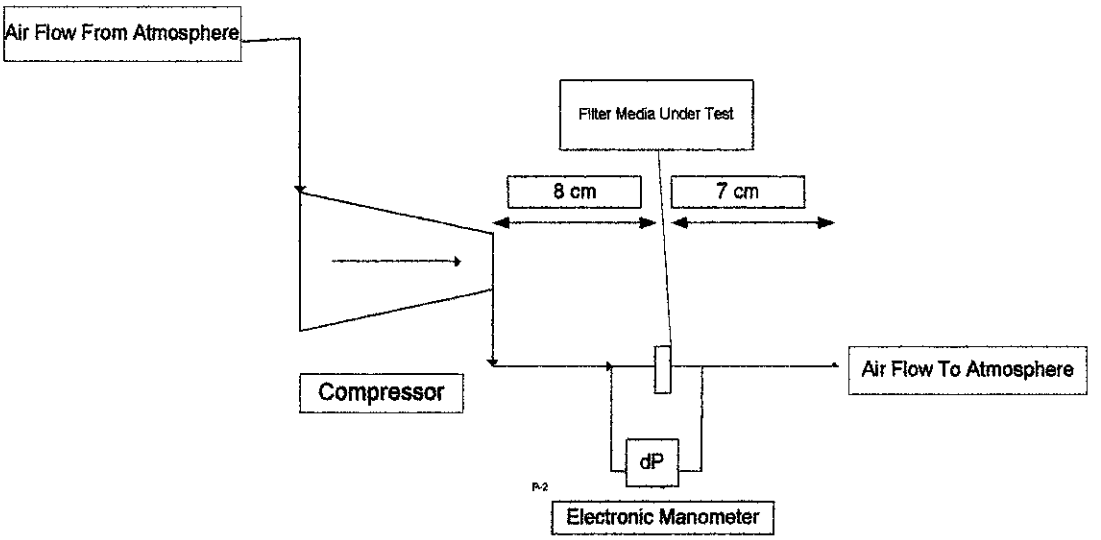

Figure 10: Gas Flow Test Set-up

3.4 SAFETY PRECAUTIONS

Safety precautionary steps are employed throughout the experiments to ensure health and safety of the author and others are not endangered. The following personal protective equipments were worn while conducting the experiments:

3.4.1 Laboratory Coat and Covered Shoes

Both equipments are worn at all times when in the laboratory.

3.4.2 Rubber Gloves

The gloves are essential especially when loading the sample in the SEM sample chamber

3.4.3 Ear Muff

The equipment is important when operating the compressor as compressor sound is very high at high frequency.

CHAPTER 4

RESULTS AND DISCUSSION

The Scanning Electron Microscope and gas flow test was selected in order to achieve the objectives of the research project, which are to develop test methods for porosity and permeability measurement in fibrous filter media and also to study the characteristics of the media itself. In order to investigate these characteristics, three samples of resin impregnated paper filter media rated 10, 28 and 50 micron, which are manufactured by a local company have been used. In addition, it is important to employ a commercialized filter media in this research in order to further investigate its behavior and compare the values with other commercialized range of values available, such as the porosity values.

4.1 FILTER MEDIA STRUCTURE AND CHARACTERISTICS

The objective of this part of the experiment is to study on the microscopic behavior of the filter media. Scanning Electron Microscope (SEM) provides the detail topographic view of the internal structure of the surface of the filter medium and further enables the evaluation of its characteristics.

For each of the samples, 10, 28 and 50 micron, different magnifications are being used in order to get the desired view of the structure. It is important to adjust the magnification during sample imaging as the wrong magnification will result in inefficiency of sample image produced. As for the 10, 28 and 50 micron samples, magnifications of 166X, 177X and 155X are employed, respectively to get clearer results and view on the pores. The results are shown in Figures 11, 12 and 13.

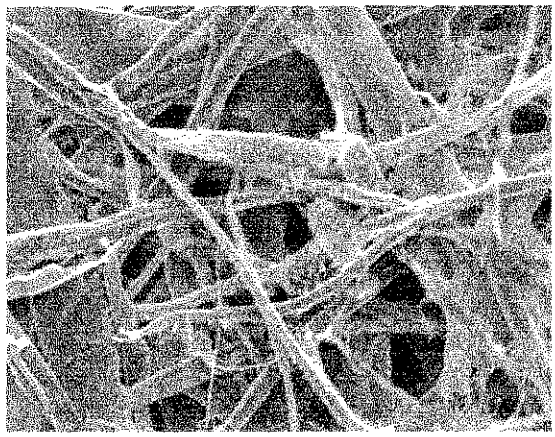

Figure 11: Structure of 10 micron sample

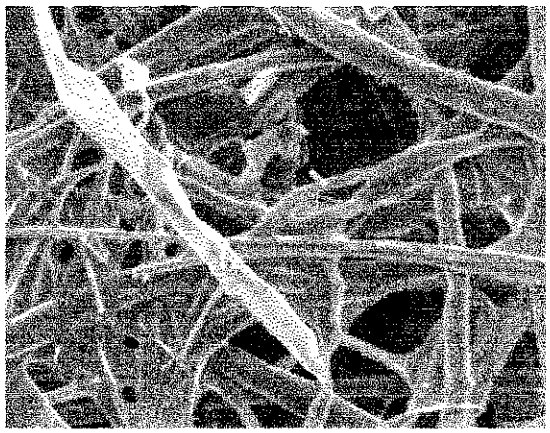

Figure 12: Structure of 28 micron sample

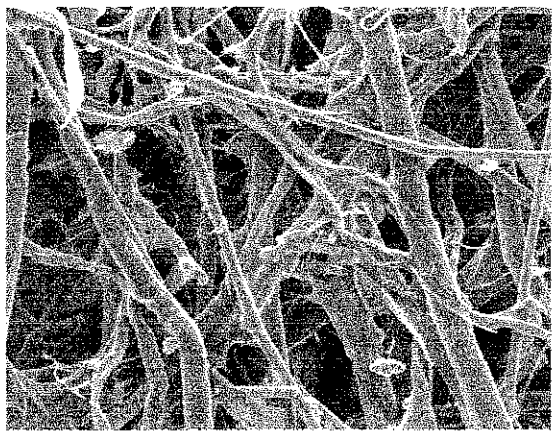

Figure 13: Structure of 50 micron sample

By observing a fibrous filter medium macroscopically, there are no distinguishable characteristics that can differentiate it from a net or sieve. Although both fibrous filters and nets have the same basic purpose, their methods of action are different. From the microscopic images shown in Figures 11, 12 and 13, it can be seen that the

filter media internals are consists of large number of fiber layers, each sparsely populated and distributed throughout the length, width and thickness. Points of fiber-fiber contact are relatively infrequent as they are randomly stacked with each other and with variety of orientations.

Compared to a net or sieve, a net will be 100% efficient in capturing particles that are larger than its perforations and the captured objects will be in contact with a substantial part of the structure on the net. Meanwhile, as for a fibrous structure as shown in Figures 11, 12 and 13, if a single layer of the fibers has a low capture efficiency, the filter as a whole can still perform well as multiple layers provide different resistance to flow for particulate that flows through. This phenomenon is called the tortousity of the filter media. As the particulate flows through the filter medium, the different flow paths of fibers at different layers throughout the thickness of the medium forces the particulates to change its direction of flow and when this happens continuously, the particulate can be captured by the mechanisms described earlier in Section 3.1. This shows that they are able to capture particles that are relatively too small to be sieve out. In fact, thick fibrous filter media are more efficient than thin ones but no fibrous filter is 100% efficient [6]. So, it can be seen that the fiber dimensions and overall layers of the fibrous filter media are essential during filtration process.

Hence, from the microscopic point of view for the filter media structure, a relationship between two important parameters can be seen, which is *layer efficiency and single-fiber efficiency*. If a fiber in a filter is oriented at right angles to the flow, the area that it presents is equal to the product of the length and the diameter of the fiber. By definition, fiber efficiency is unity when it removes from the air all of the particles that would lie within the volume swept out by its area and the velocity vector of the air, assumed to be flowing uniformly [6]. However, a fiber does not always remove 100% of the particles and the single fiber efficiency, which is defined by the quotient of the number of particles actually removed and the number that would be removed by a 100% efficient fiber. Theoretically, both single fiber and layer efficiencies are related by fiber diameter and packing fraction of the fibers (total length of fiber in unit volume of filter medium). In fact, from theoretical

definitions and by observing the fiber arrangements, it can be seen that fiber orientations are indeed important in determining the efficiency during filtration.

In addition, it can be seen that the fibers are much longer than the thickness of the filter media. The fibers tend to lie in or close to the plane of the paper. This factor is also affect the packing fraction of the fibers and would also affect the efficiency of particulate removal during filtration.

Hence, microscopically observing the filter media enables description of fibrous filter structure and also the prediction of fibrous filter media efficiency behavior towards filtration process and performance.

4.2 FILTER MEDIA POROSITY

In this research project, there are three distribution of pores that can be deduced from a filter medium, which are *surface distribution, volume distribution and also fluid-flow distribution.* From these three parameters, two are selected, which are the first and third. For evaluating porosity of the filter media samples, surface distribution is employed because it is very interesting to apply the theory stated in *Flatland* (Abbott 1963) and then compare the values with common industrial porosity range. Based on the Scanning Electron Microscope (SEM) images acquired, the porosity was calculated using *ArcView GIS 3.2 Software.*

Figure 14 shows the calculated total area of the sample taken for 10 micron filter media sample, meanwhile Figures 15, 16 and 17 are the areas considered as the number of open pores on the samples (*refer Appendix 12* for 28 and 50 micron samples images). From both values, the porosity is deduced from their ratio. *Appendix 13* shows the detail porosity calculations for all the samples.

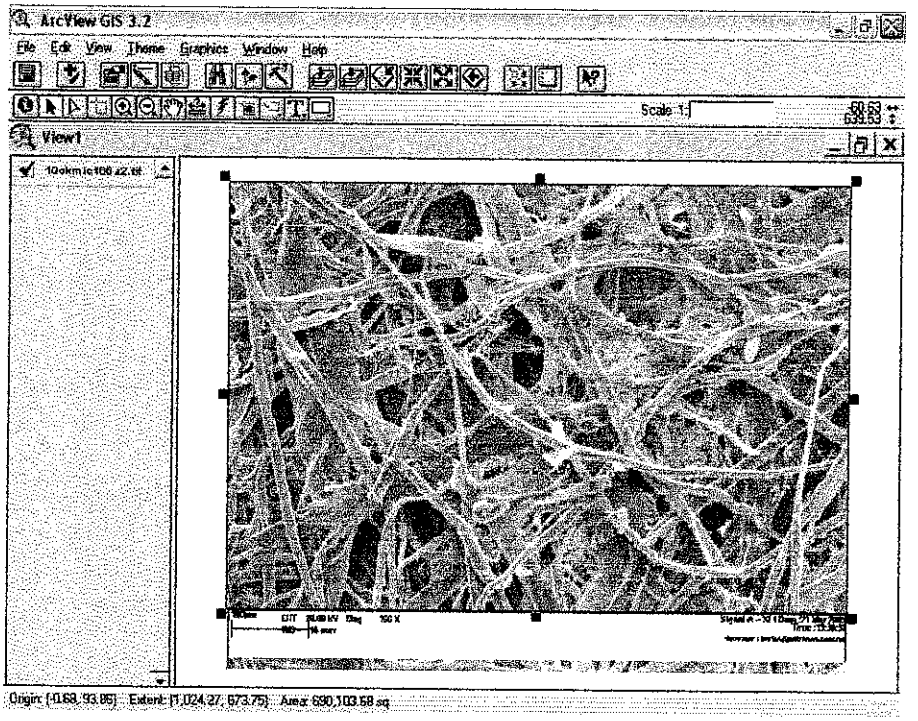

Figure 14: Calculation for Total Area for 10 micron Sample

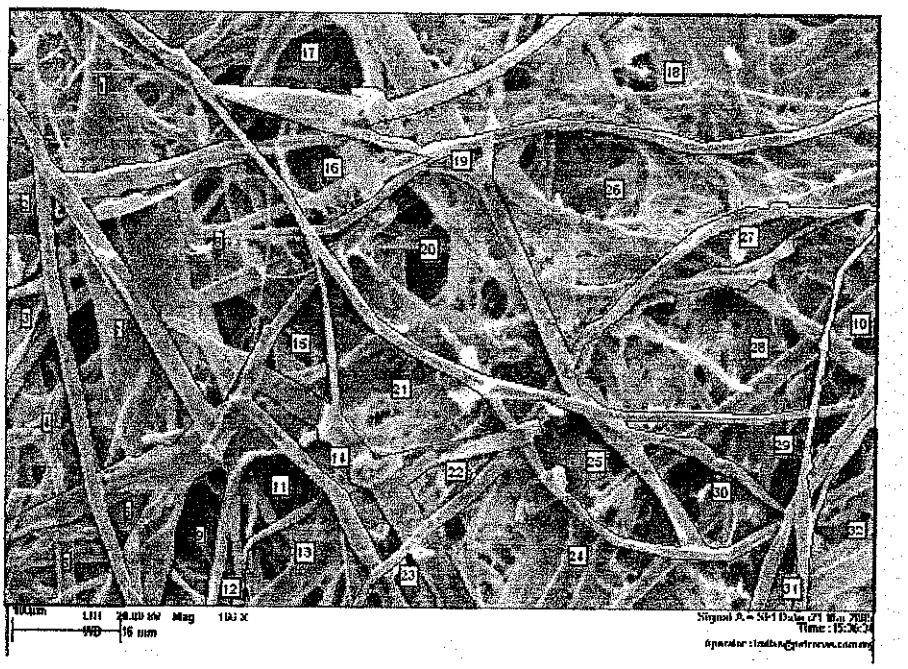

Figure 15: Sample 1 Calculation of Total Area of Pores for 10 micron

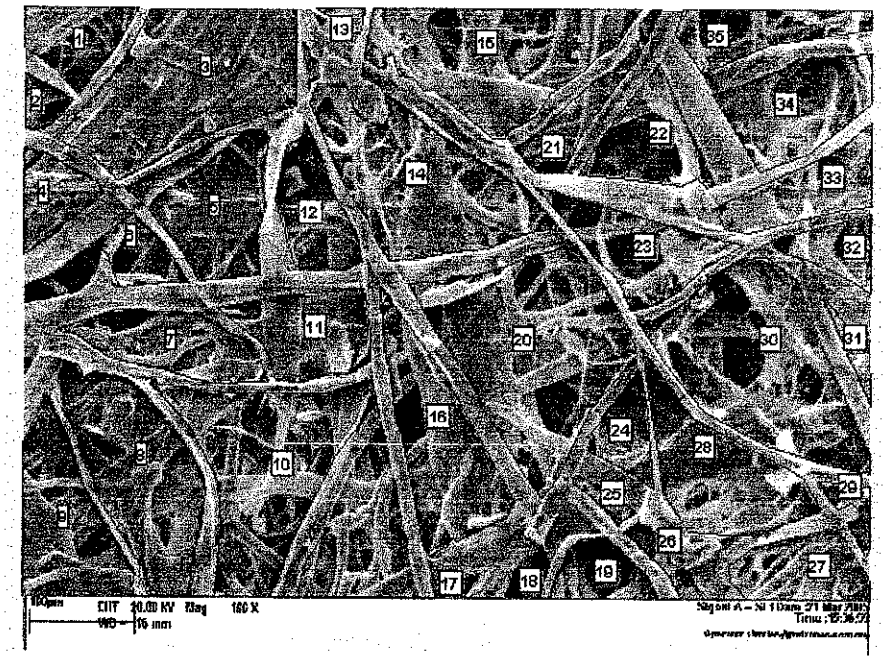

Figure 16: Sample 2 Calculation of Total Area of Pores for 10 micron

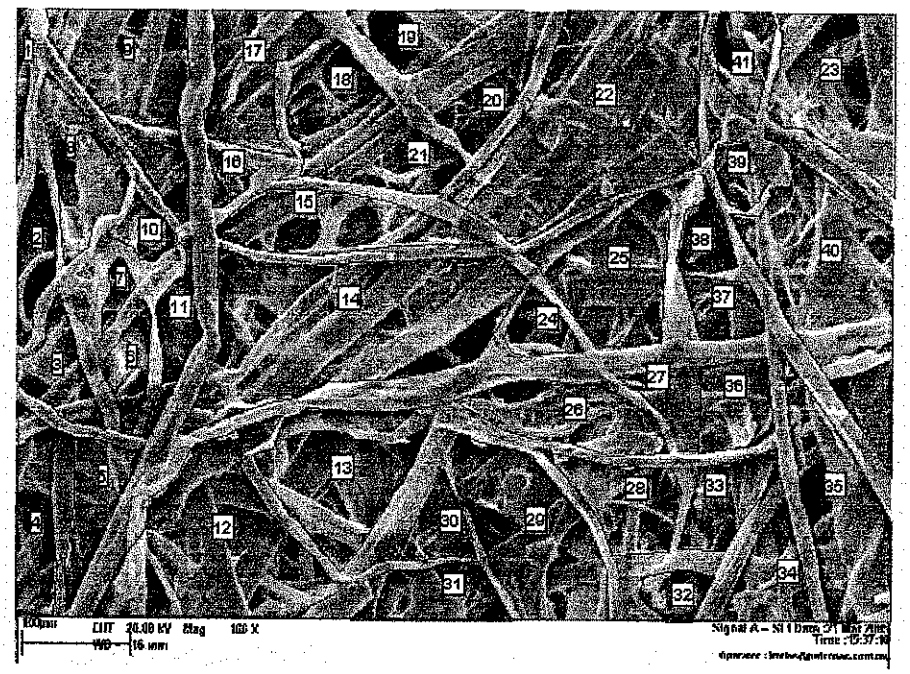

Figure 17: Sample 3 Calculation of Total Area of Pores for 10 micron

It is crucial to address that these calculations are based on the assumptions that *the pore size distribution in one layer is the same as the next layer; however, a large pore in one layer does not necessarily lie in the same spot on the next layer.* The total open spaces area is calculated in order to get the porosity by using the equation:

$$Porosity = \frac{TotalAreaofOpenSpaces}{TotalAreaof\,\mathrm{Im}age} \qquad (11)$$

It can also be said that the porosity calculations for this experiment is based n average values of the various pore size distribution on the filter media. As stated in Section 3.3.1, considering how a fluid flow through these types of media defines different paths or tunnels, where each path's diameter varies along the length. Also, different tunnels have different lengths, where as been stated earlier, the average length of the tunnel is greater than the thickness of the medium. Thus, it is important to state an average pore size by considering and average of many distributions [5].

From the calculations, the **average porosity of 10 micron, 28 micron and 50 micron** samples ***64.07%, 55.59%*** *and* ***67.29%,*** respectively. From *Appendix 5*, the typical theoretical range of porosity for fibrous materials, such as cellulose paper and filter sheets is 60-95%. The calculated values from the experiment gives reasonable results as most of them are in the theoretical range.

In addition, there is also no relationship between filter media size rating and porosity that can be determined from the experiment as the porosity values calculated shows random values for all three samples. Hence, this meets the theoretical explanation that the randomly oriented fibers in these types of filter media provide random values of porosity for different sizes/ratings. This also shows that the filter samples have open structure, which theoretically indicates that they offer low resistance to fluid flow.

4.3 GAS FLOW TEST

Another distribution that can be employed to calculate the pore size of a randomly oriented fibrous filter media is the fluid-flow distribution. Hence, the experiment is done by applying the industrial Frazier Test to a laboratory scale test. The important parameters taken into account while conducting the experiment were the pressure drop across the filter media and also the downstream velocity of the filter media. Both these parameters are used to plot a graph which further determines the flow average pore diameter and other important parameters of the filter media samples.

As been stated in Section 3.4.3, the experiment is aimed to obtain a straight line graph which is similar to Line 1 in Figure 6, where the region of interest lies of the slope equals to 1. In this region, it can be seen that the flow is laminar (viscous). Theoretically, viscous drag is the predominant resistance to flow. At higher velocities, where the slope in Figure 6 equals to 0.5 shows the symptom of inertia flow, in which the liquid is constantly asked to change direction of flow where viscous drag constitutes a relatively small resistance to flow. Laminar flow is the kind of fluid-velocity profile that can be seen in a pipe: the greatest velocity in the center, and the velocity falls, approaching zero towards the wall. In fact, filtration is usually done in laminar flow region, where the pressure drop and velocity are direct functions of one another; hence, the inertia term is negligible. Thus, the inertia term value is not of interest in this experiment [5].

Figures 18, 19 and 20 show the experimental results for each of the samples (*refer Appendix 14* on the detail calculations). All the graphs show straight line behavior accordingly to the theoretical trend in Figure 6. However, the slopes of the graphs, which are 0.8346, 0.694 and 0.6883 show slight deviation from the theoretical value, which is 1. Another deviation that can be observed is the region of the graphs where the logarithmic of downstream velocity is in the negative region. This is due to the low velocity values because the experiment is done on laboratory scale. In order to achieve laminar flow for the 3 cm diameter pipeline, low velocity needs to be employed so that the air flow can be maintained and does not reach turbulent region for its Reynolds numbers. As an overall, the theoretical equations pertaining to the graph can still be applied for this experiment as the graphs shows reasonable trends.

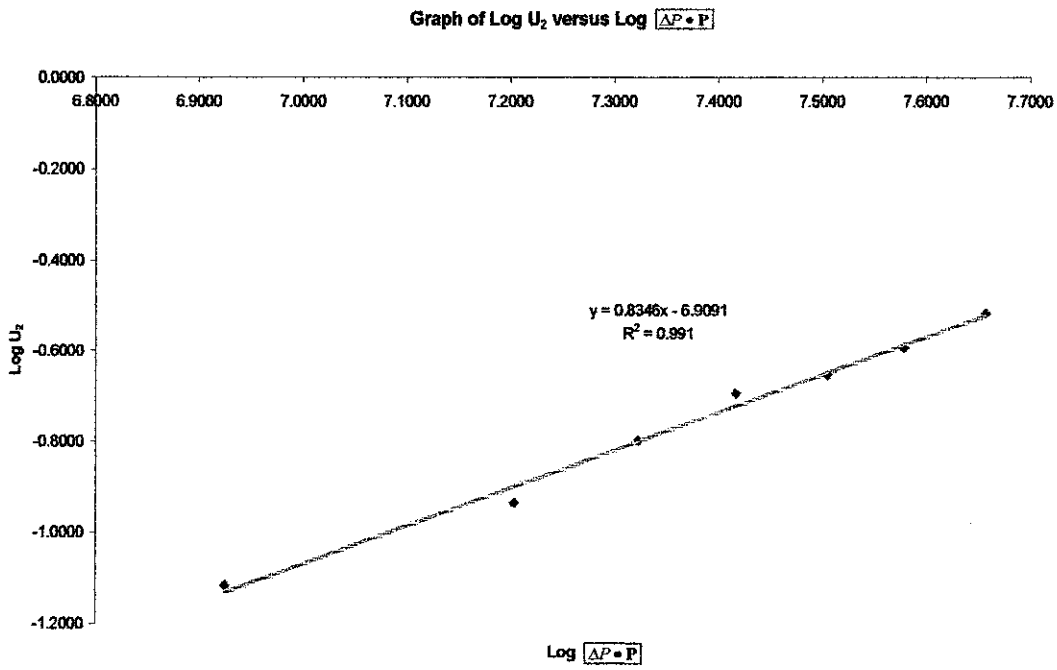

Figure 18: Graph of Log U_2 versus Log ΔP.P for 10 micron Sample

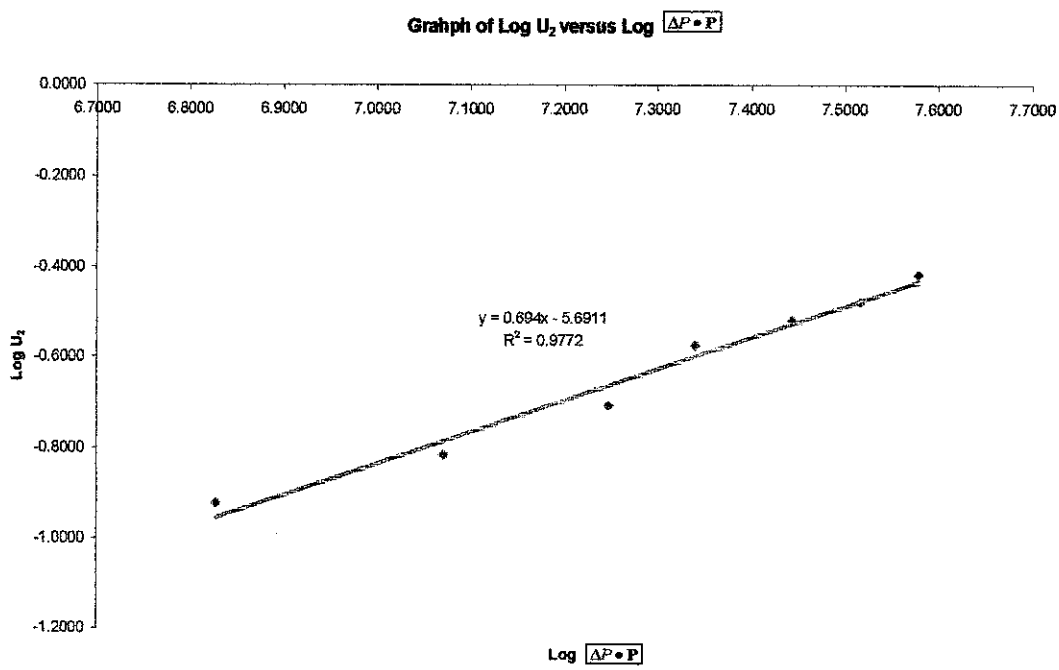

Figure 19: Graph of Log U_2 versus Log ΔP.P for 28 micron Sample

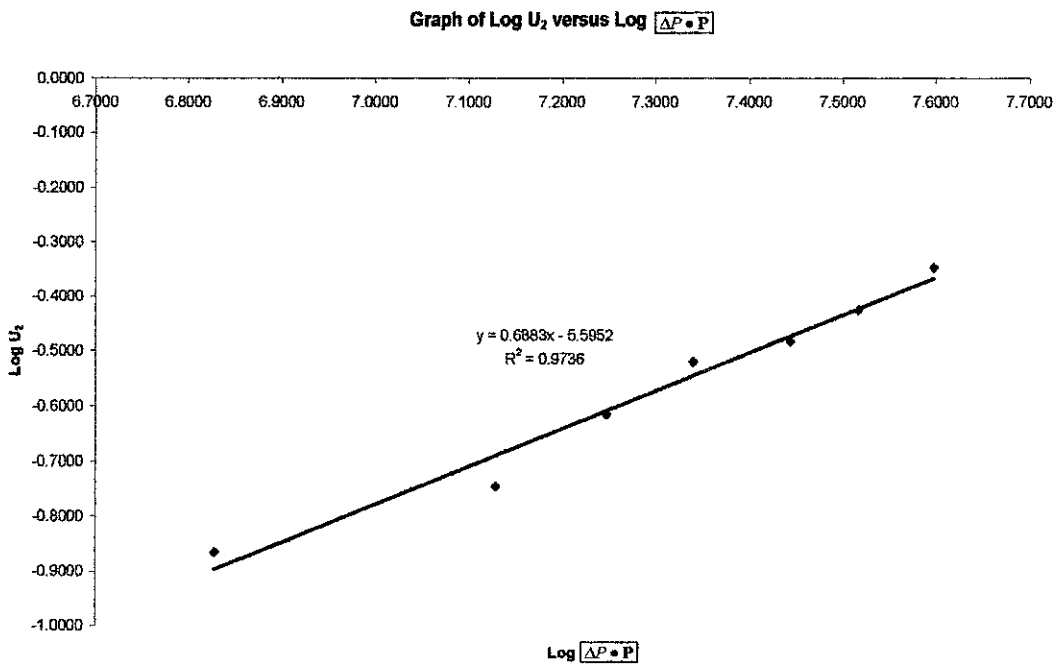

Figure 20: Graph of Log U_2 versus Log $\Delta P.P$ for 50 micron Sample

Referring to Appendix 14, related calculations are done to obtain the values for average permeability coefficient, $k_{v,ave}$, flow average pore diameter, d_p, permeability, specific pore diameter, d, fiber diameter, d_f and also average viscous-term coefficient, α_{ave} . Those values are tabulated in Table 1.

Filter Media Size / Calculated Values	10 micron	28 micron	50 micron
Average permeability coefficient, $k_{v,ave}$, m^2	5.79117×10^{-12}	1.43391×10^{-11}	1.74068×10^{-11}
Flow average pore diameter, d_p, micron	21.62	33.75	37.18
Permeability, $\frac{m^3/s}{m^2 Pa}$	7.291×10^{-4}	1.235×10^{-3}	1.390×10^{-3}
Specific pore diameter, d, micron	30.48	50.09	51.94
Fiber diameter, d_f, micron	17.09	40.02	25.25
Average viscous-term coefficient, α_{ave}, m^{-2}	1.6794×10^{11}	7.0139×10^{10}	5.7815×10^{10}

Table 1: Calculated Values for 10, 28 and 50 micron Samples

From the experiment, five filtration specific values are determined by using the Darcy Equation and Kozeny-Carman relationship for porous filter media. Referring to Table 1 and Figure 21, the permeability and permeability coefficient values are seen to be directly proportional with the filter rating/size. The *permeability values increases as the filter sizes increases* because as the size of open pores increases, the fluid tends to flow more easily. In other words, the *ease of flow of fluid increases with increasing size of open pores.* Hence, pore size distribution provides higher area of flow for fluid.

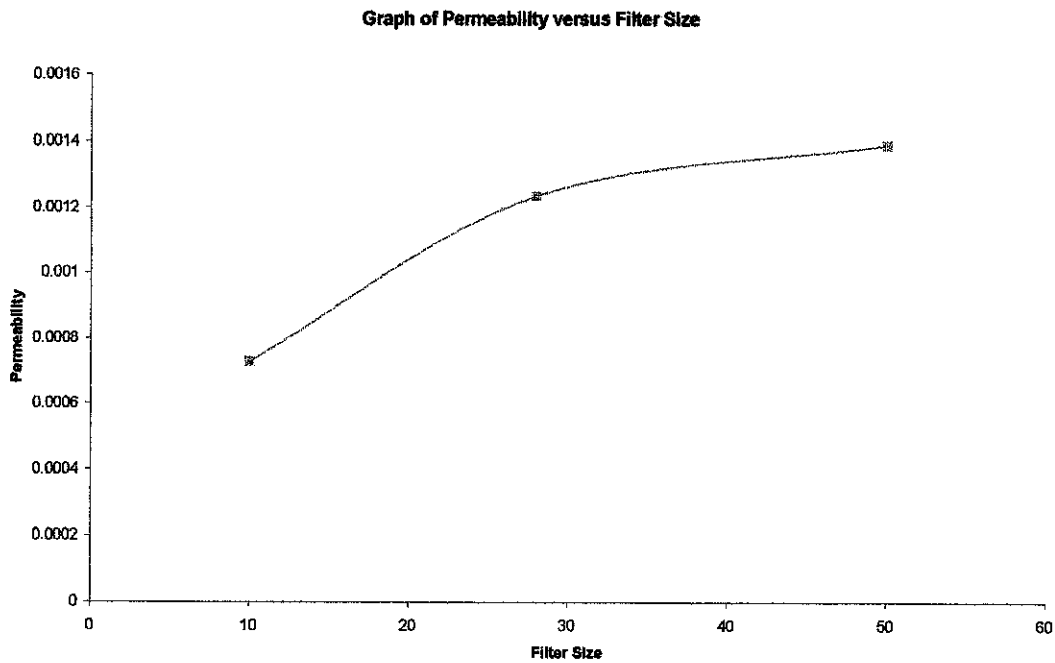

Figure 21: Graph of Permeability versus Filter Size

Specific diameter, d is the internal diameter of pores considered as a tube with length. *L.* The difference between specific diameter and flow average pore diameter is that the flow average pore diameter is taken from the permeability (flowability) characteristics of the filter medium, meanwhile the specific diameter values depends of the Kozeny-Carman constant for fibrous filter media, which depends on the porosity of the filter media. The values of flow-average pore diameter and specific diameter for all the samples show variation of values with the original rating of the samples, which are 10, 28 and 50 micron. This is due to the variation on the fiber orientation and arrangements that resulted in the variations of the results. However, the values show increment for the increment of the filter size.

As stated in Section 3.3, the relative efficiencies of fibrous filter media are a function of fiber diameter. The narrower the fibers, the closer they are compacted resulting in smaller flow paths, providing better filtration efficiency. Theoretically, the fiber diameters tend to increase with the increment of filter media ratings. However, from the experiment, the fiber diameter values depend on the specific diameter of the pores and also the porosity. The values increases as goes from 10 micron to 50 micron but shows very high value at 28 micron. This deviation is most likely caused by the variation on the porosity value, which varies depending on the fiber arrangement.

Another parameter that can be deduced from the experiment is the viscous-term coefficient, α. From Table 1, the viscous-term coefficient values decreases as the filter media rating increases. This relationship is reasonable because the term is inversely proportional to permeability coefficient and permeability values as shown in Equation (3) and Table 1. In addition, this relationship can also be seen from the decrement of slope values (which represents the viscous-term) as the filter size increases shown in Figures 18, 19 and 20.

4.4 EXPERIMENTAL ERRORS

There were few difficulties during the research that would probably produce some errors in the results:

4.4.1 Non-homogenity of Filter Media Under Test

Having a non-homogeneous property, the filter sample imaging gives various trends and patterns of fibers for each image taken. Thus, the pore size distribution is also wide throughout the sample. This produced difficulties in determining the accurate average porosity of the samples when evaluating each pores as the research applies surface distribution only and not accounting the effect on the pore diameter variations along the filter media thickness.

4.4.2 Determination of the Pores on the First Layer

With various distributions of pore sizes and random array of fiber arrangements, it is difficult to accurately plot and determine accurately the first layer of pores according to the fiber arrangements.

4.4.3 Measurement of Velocity

Inaccurate velocity measurement during the gas flow test could lead to deviation on the results. This is because the velocity profile for laminar flow is at maximum in the center of the pipe and at maximum when reaches the wall.

4.5 CORRECTIVE ACTIONS TAKEN

From the overall flow of the research project, few corrective actions can be taken to improve results.

4.5.1 Pre-test to Obtain Correct Magnification

A pre-test was done for sample imaging using Scanning Electron Microscope. During the pre-test, few magnifications for the samples were taken. This is to ensure that the correct magnification is done for each of the samples in order to get the correct view for sample analyzing.

4.5.2 Repeating the Experiments

It has been the most convenient and important practice *to repeat each of the experiments done* in order to compare and take the average values of the results in order to make sure that the results obtained are higher in accuracy.

4.5.3 Data Taken at Steady State Values

During the gas flow test, the values for downstream velocity and differential pressure are taken at steady state values in order to make sure that the system is already stabilizes.

4.5.4 Careful Velocity Measurement

The readings for velocity measurement are carefully taken for each experiments by taking the values at steady state and also carefully pointing the anemometer sensor towards the center of the pipeline not allowing it to move for each readings.

CHAPTER 5

CONCLUSION AND RECOMMENDATIONS

The main purposes of the research project are to experimentally develop test methods for evaluating filtration-specific properties of the resin impregnated paper filter media. It has been known that fibrous filter media are depth type filtration application in the industry. Although these types of filter media are thin, they provide tortuous path to contaminants in a fluid and also provide low resistance to flow especially for air filtration applications.

The filter media samples obtained, which are rated 10 micron, 28 micron and 50 micron being tested by surface distribution using Scanning Electron Microscope (SEM) imaging and fluid flow distribution using Gas Flow Test to determine its porosity also other related properties such as permeability and also average pore diameter values.

The results obtained from the research shows that

- Fibrous filter media internals are consists of large number of fiber layers, each sparsely populated and distributed throughout the length, width and thickness with relatively infrequent points of fiber-fiber contact as they are randomly stacked with each other and with variety of orientations.
- Porosity values are independent of the filter sizes for fibrous filter media as the pores in fibrous filter media are randomly oriented.
- Permeability values increase as filter media size increases which show that the ease for fluid flow increases as the sizes of open pores increases.

From several experiments that have been performed, objectives of this research have been achieved. However, additional study and research have to be conducted in order to enhance the knowledge on fibrous filter media characteristics for

improvement of fibrous filter media knowledge and expanding its applications. Few recommendations for future researchers are:

- To study the volume distribution of the pores of fibrous filter media in order to account for the filter media thickness for porosity measurement.
- To conduct laboratory scale multi-pass test in order to relate the porosity values with the filter media efficiency that is useful for further prediction of filter media filtration-specific properties.
- To study on other properties besides filtration-specific properties, such as the machine-orientated and application-orientated properties for further enhancement on each of the properties' effect on filtration effectiveness.

REFERENCES

1. Purchas, Derek B. and Sutherland, Ken. *Handbook of Filter Media*, 2nd Edition, Elsevier Advance Technology. 2002
2. Matteson, Michael J. and Orr, Clyde. *Filtration Principles and Practice*,. 2nd Edition, 1987
3. Purchas, D. B., *Industrial Filtration of Liquids*, Leonard Hill, London, 1967
4. Dickenson, T. Christopher. *Filters and Filtration Handbook.* 4th Edition. Elsevier Science Limited, New York, 1997
5. Johnston, Peter R. *A Survey of Test Methods in Fluid Filtration*, Gulf Publishing Company, Houston, Texas. 1995
6. Brown, R. C., *Air Filtration: An Integrated Approach to the Theory and Applications of Fibrous Filters*, Pergamon Press, 1993
7. Ramstorp, Matts, *Contamination Control in Practice: Filtration and Sterilisation*, Wiley VCH Gmbh & Co. 2003
8. Rossiter, Bryant W. and Hamilton, John F. *Physical Methods of Chemistry, Volume VI: Microscopy.* 2nd Edition. John Wiley and Sons, New York. 1991
9. Wakeman, R. J. et. al., *Filtration: Equipment Selection and Process Simulation*, Elsevier Science Limited, 1999
10. Geankoplis, C. J., *Transport Processes and Separation Process Principles*, 4th Edition, Prentice Hall, 2003
11. Perry, R. H. et. al., *Perry's Chemical Engineers Handbook*, 7th Edition, McGraw Hill, 1997
12. Scanning Electron Microscope Model LEO 1430VP Manual
13. Cybron Asia Compressible Flow Bench Manual
14. Pall Corporation
15. www.leo-usa.com
16. www.sciencedirect.com

APPENDICES

APPENDIX 1: Typical Filter Media Types

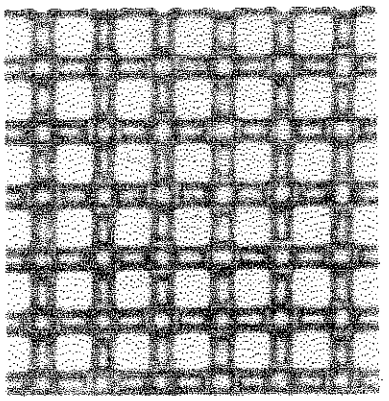

FIG. 1 (a)

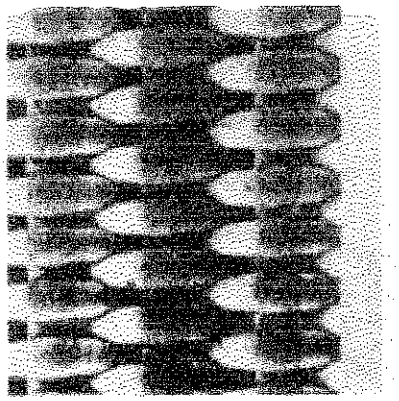

FIG. 1 (b)

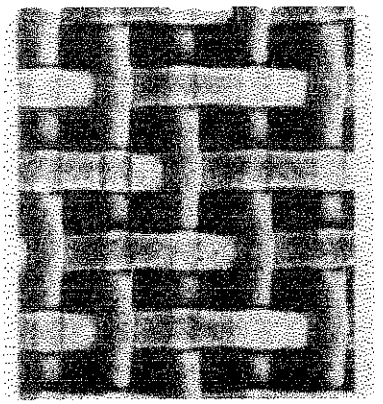

FIG. 1 (c)

FIG. 1 (d)

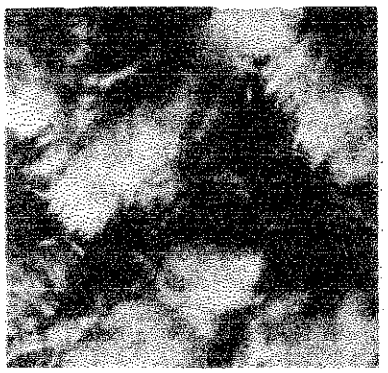

FIG. 1 (e)

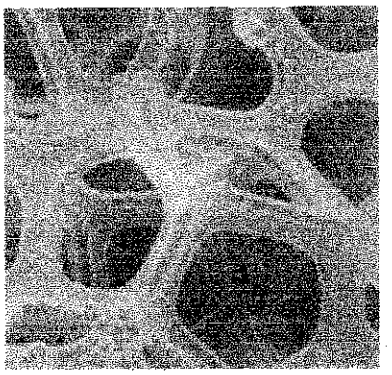

FIG. 1 (f)

FIG. 1 Typical filter media: (a) plain-weave monofilament [93], (b) Reverse-plain-dutch-weave monofilament [89], (c) twill-weave monofilament [89], (d) Plain-weave multifilament, continuous fiber [88], (e) plain-weave multifilament, staple fiber [93], (f) porous metal foam [90], (g) glass fiber-cellulose fiber blend [91], (h) multifilament twill weave [88], (i) wool felt cloth [88], (j) Nucleopore membrane [92].

FIG. 1 (g)

FIG. 1 (h)

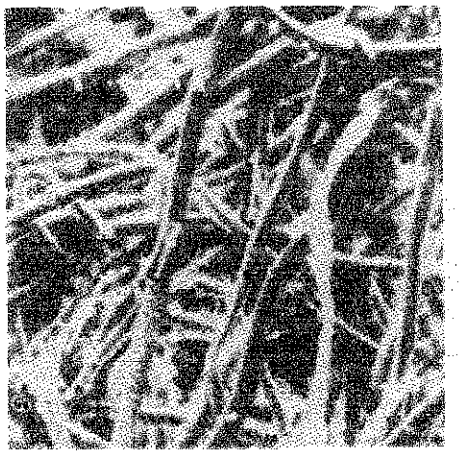

FIG. 1 (i)

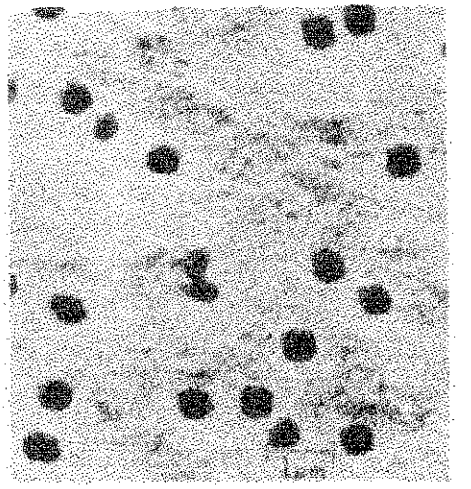

FIG. 1 (j)

APPENDIX 2: Properties of Filter Media

Table 1.4 Machine-orientated properties

1	Rigidity
2	Strength
3	Resistance to creep/stretch
4	Stability of edges
5	Resistance to abrasion
6	Stability to vibration
7	Dimensions of available supplies
8	Ability to be fabricated
9	Sealing/gasketing function

Table 1.5 Application-orientated properties

1	Chemical stability
2	Thermal stability
3	Biological stability
4	Dynamic stability
5	Absorptive characteristics
6	Adsorptive characteristics
7	Wettability
8	Health and safety aspects
9	Electrostatic characteristics
10	Disposability
11	Suitability for reuse
12	Cost

Table 1.6 Filtration-specific properties

1	Smallest particle retained
2	Retention efficiency
2.1	The structure of filter media
2.2	Particle shape
2.3	Filtration mechanisms
3	Resistance to flow
3.1	Porosity of media
3.2	Permeability
4	Dirt-holding capacity
5	Tendency to blind
6	Cake discharge characteristics

APPENDIX 3: Factors Effecting the Retention Rates of Depth Filters

Factors affecting the retention rates of depth filters			
Mechanical factors		**Adsorptive factors**	
Product	**Depth filter**	**Product**	**Depth filter**
● Nature of the impurities/particles ● Number and size of the impurities/ particles ● Viscosity ● Chemical composition	● Void volume of the filter medium ● Structure of the three-dimensional screen ● Size of the internal surface area (dirt holding capacity) ● Thickness of the filter medium ● Nature, upgrading and composition of the individual material components	● Chemical composition ● Charge of the impurities/particles ● Concentration of the impurities/ particles ● pH-value ● Flow velocity ● Polarity of the impurities/particles ● Temperature	● Structure of the three-dimensional screen ● Number of the charge carriers ● Nature of the charge carriers ● Magnitude of the charge ● Polarity of the charge carriers

APPENDIX 4: Typical Costs of Various Types of Filter Media

Class	Type	Cost (£/m²)
Cellulose paper	Resin impregnated	0.25–0.5
	Unimpregnated	0.15–0.25
Glass paper		0.4–0.8
Filter sheet	Asbestos free	4–6
Membrane	Acrylic copolymers	60–100
	Cellulose	45–75
	Cellulose esters	90–150
	'Nuclepore' polycarbonate	125–220
	Nylon	70–130
	Polyethersulphone	75–140
	PTFE on polypropylene substrate	400–500
	UF membranes	75–135
Mesh (monofilament)	Polyamide (5–200 μm)	20–95
	Polyester (5–200 μm)	20–100
	Stainless steel (5–100 μm)	35–175
Needle felt	Staple fibre	3–7
	Polyamide	5–7.5
	Polypropylene	4–5
Non-woven: spunbonded	Polyester	0.1–2.5
	Polyethylene	0.1–3
	Polypropylene	0.05–2
Non-woven: melt blown	Polyester	0.2–3
	Polypropylene	0.1–2.5
Porous ceramic	25 mm thick	200–300
Precoat powder	Coating 0.6 kg/m²	0.25–0.4
Sintered stainless steel	Powder (1.6 mm thick)	260–380
	Metal fibre (0.8 mm thick)	250–360
	Mesh (5 layer)	700–1200
Woven fabric	Cotton	5–7.5
	Polyamide – multifilament	5–7.5
	Polyamide – staple	6–8.5
	Polyester – multifilament	4–6
	Polyester – staple	5–8.5
	Polypropylene – multifilament	4–6
	Polypropylene – staple	5–7.5
	Aramid (filament warp/staple weft)	12.5–15
	Glass (filament warp/staple weft)	5–8
	PTFE	35–40

APPENDIX 5: Typical Porosities of Filter Media

	% free area
Wedge wire screen	5–40
Woven wire:	
twill weave	15–20
square	25–50
Perforated metal sheet	30–40
Porous plastics (moulded powder)	45
Sintered metal powders	25–55
Crude kieselguhr	50–60
Membranes	80
Paper	60–95
Sintered metal fibres	70–85
Refined filter aids (diatomite, perlite)	80–90
Plastic, ceramic foam	93

APPENDIX 6: Examples of the Variety of Permeability Scales Formerly Used

Nature of medium	Type of permeability scale	Typical data
Sintered metals	gpm of water or cfm of air/sq ft at pressures in psi, through defined thickness (usually $^1/_8$ in) generally as graphs	5 μm pore. Δp1 psi – 25 cfm of air/ft^2 1.2 gpm of water/ft^2 20 μm pore. Δp1 psi – 48 cfm of air/ft^2 6.5 gpm of water/ft^2
Ceramics	(a) gpm of water or cfm of air at pressure in psi (b) mm Hg, either/ft^2 or per element; usually through defined thickness of about $^1/_2$ in	15–20 μm pore, (a) 100 scfm/ft^2 of air at 10 psig Δp=275 mm Hg (b) 5 gpm/ft^2 water. Δp=75 mm Hg
Woven metal	gpm of water/sq in at 1 psi	100 mesh square weave, 0.0045 in wire, 30% open area – 12.1 gpm/sq in. 47 μm dutch twill, 50 × 700–3.0 gpm/sq in
Woven fabrics	cfm of air/sq ft at 0.5 in WG	cotton twill – 3–15 cfm/ft^2 monofilament nylon – 300–900 cfm/ft^2 multifilament nylon – 5–500 cfm/ft^2 glass – 2–20 cfm/ft^2
Non-woven fabrics	(a) cfm of air/sq ft at 0.5 in WG (b) gpm of water/sq ft at 1 psi	(a) 0.5–230 cfm of air/ft^2 (b) 3–500 gpm of water/ft^2
Paper	(a) time for flow of e.g. 1000 cc water at pressure of e.g. 245 mm Hg (b) time for flow of fixed volume of air at defined pressure (c) litre of air per min/10 cm^2 at pressure of 10 cm WG (d) pressure needed to produce flow of e.g. 1 cfm/10 cm^2 (e) rate of air flow/unit area divided by pressure drop, e.g. cm/s/100 cm^2 divided by cm WG	(a) 4–100 s (b) $1^1/_2$–50 s (c) 40–400 l (d) 1–73 cm WG (e) 7.5–150
Sheets	gph of water either/ft^2 or/sheet at e.g. 10 psi	12–800 gph/ft^2
Filter aids	(a) graph showing cumulative flow/ft^2 versus time: using sugar and other solutions containing suspended solids on a batch test basis (b) expressed as ratio, relative to slowest in some range of products (c) darcies, based on water flow	(c) 0.05–5 darcies
Sand	Head loss, ft of water	

APPENDIX 7: Derivation for Tortousity Term (Johnston 1992c)

Imagine a plane in a filter medium perpendicular to the flow of fluid. On this plane, a grid is drawn, where the sizes of a single square in the grid corresponds to the size of the flow average pore. Consider that this grid has a thickness corresponding to the length of the sides of the square of the grid. That is, we have a plane of cubes, some empty (the pores) and some filled (the filter medium).

The probability, p that the cube is empty corresponds to the porosity. The probability that a cube is occupied (solid) is q, equal to $1-p$. Now, consider the flow of fluid through this grid. Consider that N slugs of fluid approach this grid, and the size of a slug equals to the size of a cube. It can be seen that Np slugs pass through the grid. That is, the distance traveled through the grid equals to the thickness.

Of those Nq slugs that hit the solid cube, and have to take a single side step, Npq do find an empty cube, and Nq^2 do not. The total distance traveled by the Npq slugs in passing through the grid is thus twice the thickness.

Of those Nq^2 slugs still on the grid, Npq^2 find an empty cube after two side steps, and thus travel a distance of three times the thickness of the grid in passing through.

Continuing this logic, the average distance traveled by all slugs, as a multiple of the grid thickness, the tortousity factor, ε is

$$\tau = \frac{N(p+2pq+3pq^2+4pq^3...)}{N} = \frac{1}{p} = \frac{1}{\varepsilon} \qquad \textbf{(ASTM 902)}$$

APPENDIX 8: Permeability Test Methods in the Industry

Appendix 8-1: Schematic for Frazier Differential Pressure Air Permeability Measuring Machine

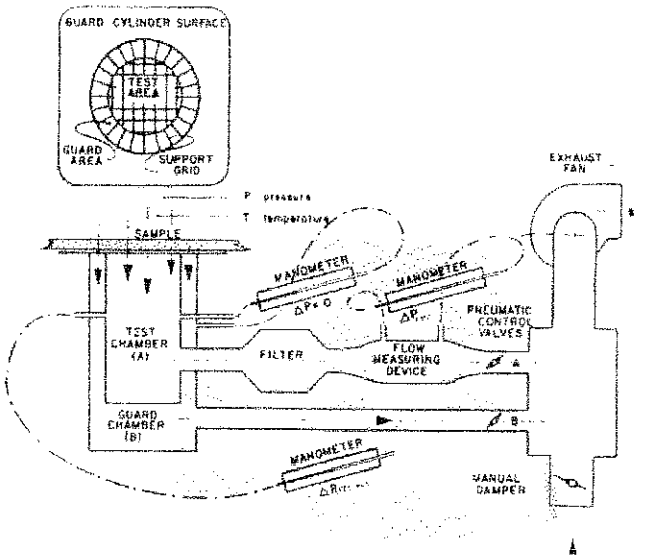

Appendix 8-2:Coulter Porometer

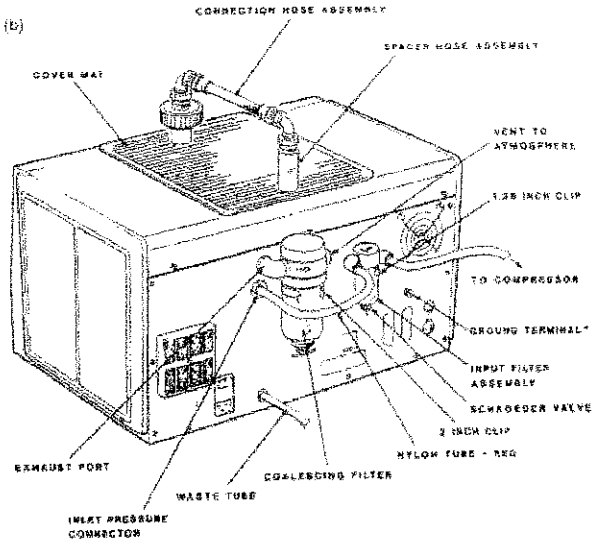

Appendix 8-3: Gurley Densometer for Measuring Air Permeability

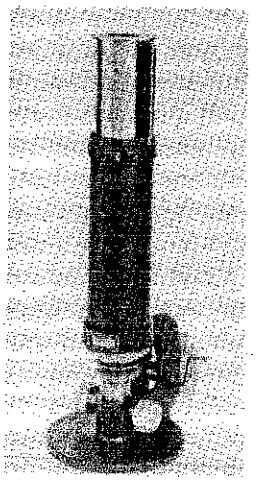

Appendix 8-3: Shirley Air Permeability Tester

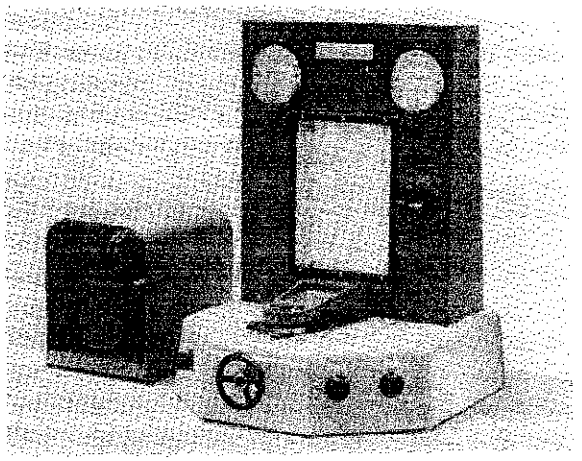

APPENDIX 9: Porosity Test Methods in the Industry

Appendix 9-1: Bubble Point Test Apparatus

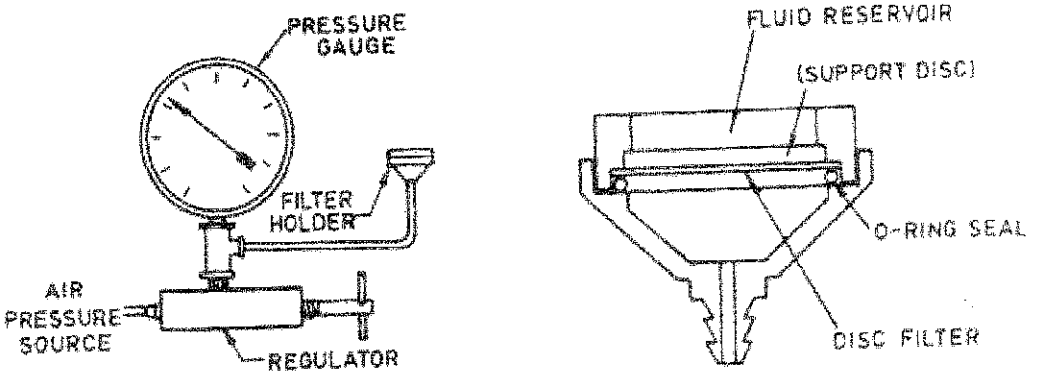

Appendix 9-2: Mercury Porosimetry

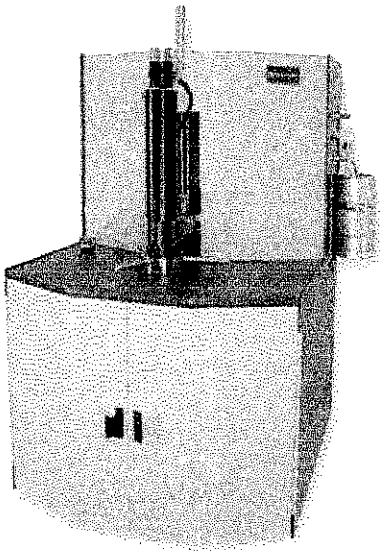

APPENDIX 10: Filter Media Samples Properties

1. **Content:** Resin Impregnated Paper.
   - 10 micron

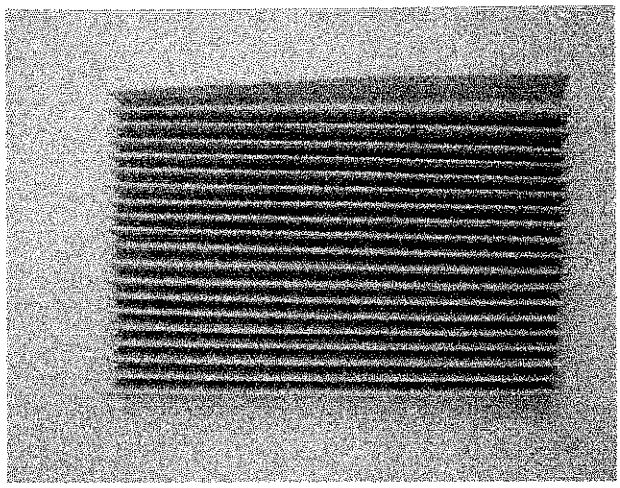

   - 28 micron

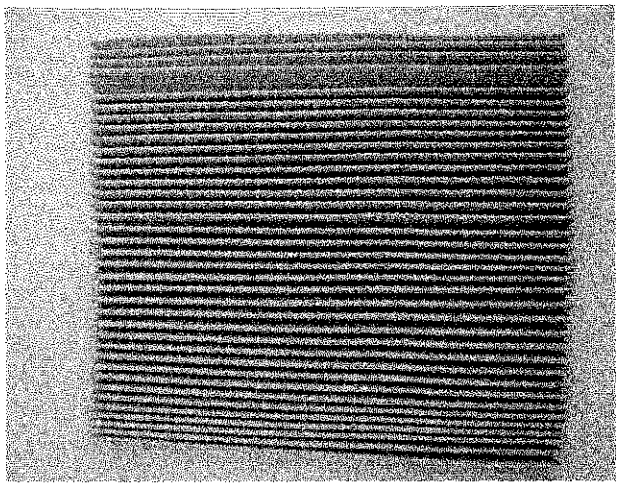

   - 50 micron

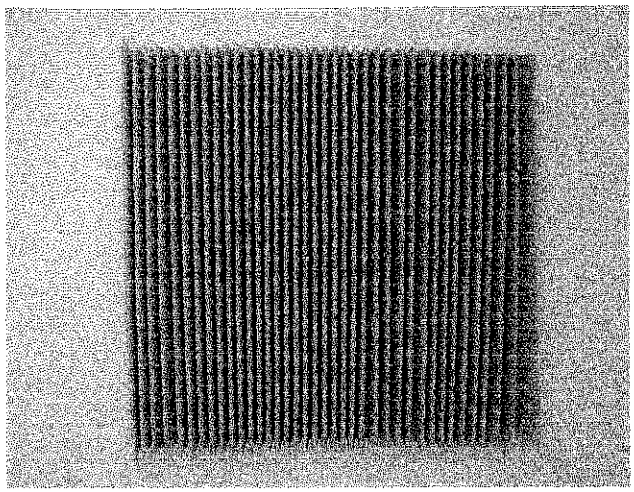

2. **Homogenity:** Non-Homogeneous

Fibre Homogenity

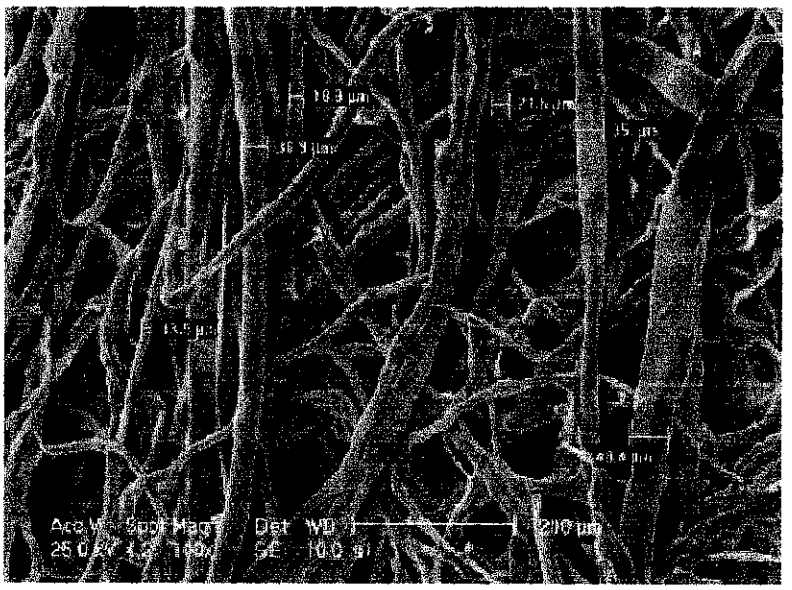

28 micron

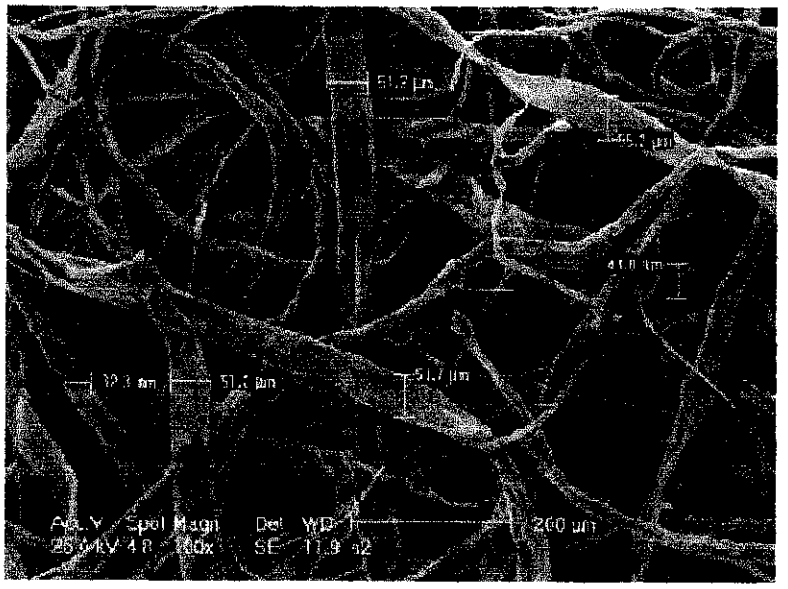

50 micron

3. **Conductivity:** Not Electrically Conductive

4. Other Properties

SAMPLE TEST REPORT

SAMPLE REFFERENCE	#10 MICRON	#28 MICRON	#50 MICRON
Basis Weight			
cured	176	191	158
Thickness at 6.7 N/cm2			
corrugated	0.65 - 0.70	0.85 - 0.90	0.80 - 0.84
Air resistance			
at 40 cm/s/10 cm2	58	3.9	1.95
Air permeability			
at 2 mbar/20 cm2	18.5	253	460

5. **Applications:** For high pressure gas streams, high pressure water injection and disposal and also for fluid processing

APPENDIX 11: Detail Scanning Electron Microscope (SEM) Procedures For Sample Imaging

1. The system is turned on to S.E mode as the user is going to used the secondary electron detector from the normal TV mode by clicking on the macro that toggles the camera view. The first signal obtained is usually just noise. The following steps are suggested to obtain an image:
    - The brightness is maximized
    - The contrast is adjusted until the image is grey
    - The magnification is decreased too lowest available.
    - Focus until see something
2. It helps to have a large object to focus on. If the user looking at a flat clean wafer with tiny features, the user might have trouble obtaining the correct focus.
3. Once an image is obtained, the region of interest is focused, the right magnification is chosen, focused, and the image is obtained either with the printer or the save image macro.
4. If the image is poor, even when the focus is optimised, a stagnation or beam alignment might be needed.
5. The EHT will also significantly impact the image. A large EHT improves resolution, but leads to deeper beam penetration.
6. If only the surface is of interest, a low EHT often works better. A lower WD also the resolution, but remember to stay above 3 mm, and always turn the camera on when moving the z-axis or tilt.

APPENDIX 12: Porosity Calculations for 28 and 50 Micron Sample

Appendix 12-1: Total Area

1. 28 micron

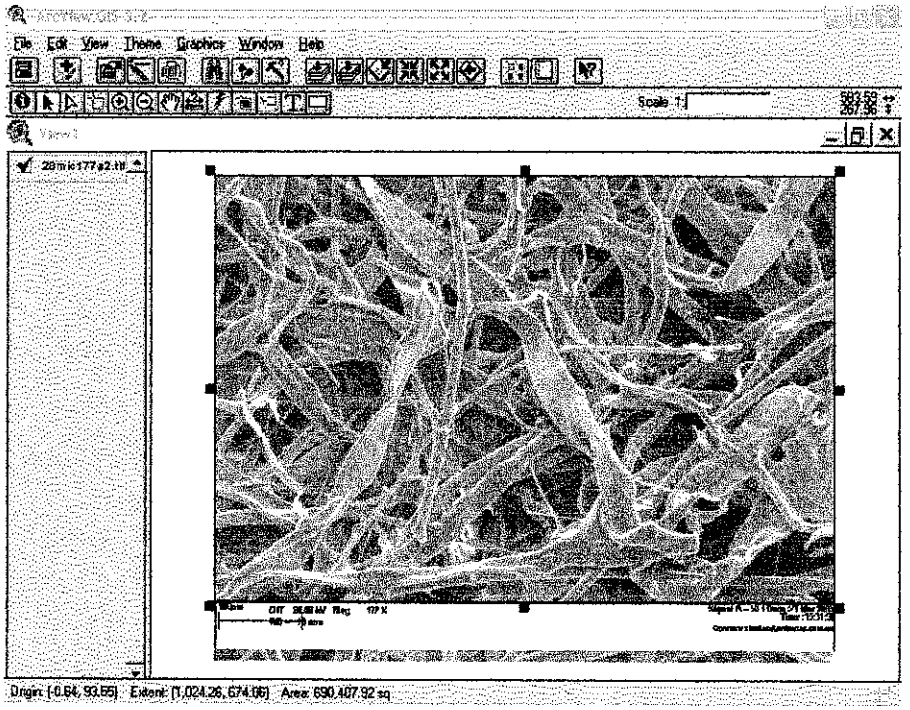

2. 50 micron

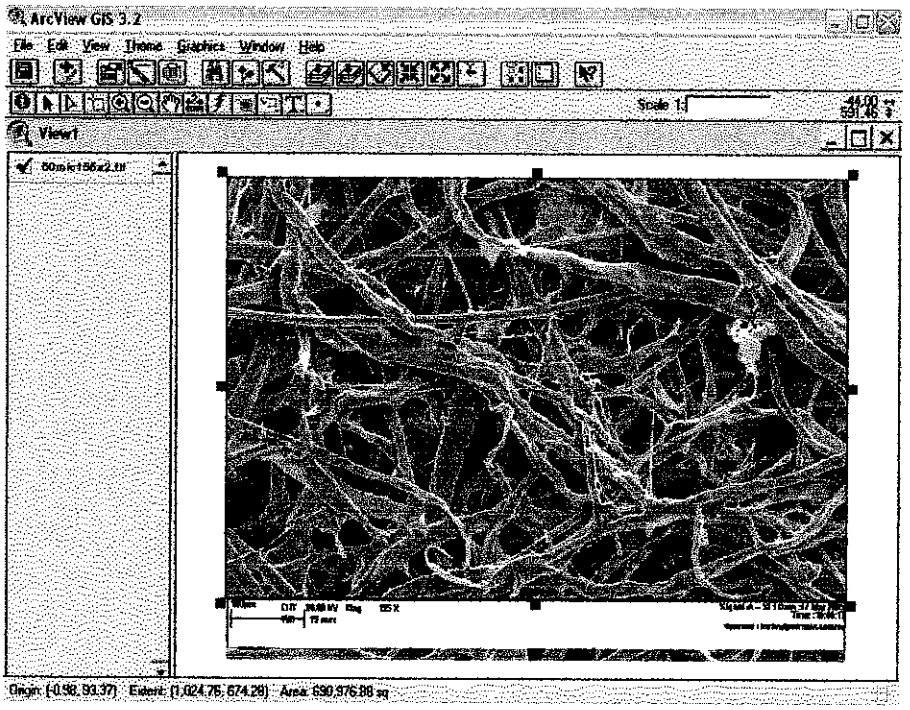

Appendix 12-2: Total Pore Size Area Calculation

1. 28 Micron

   - Sample A

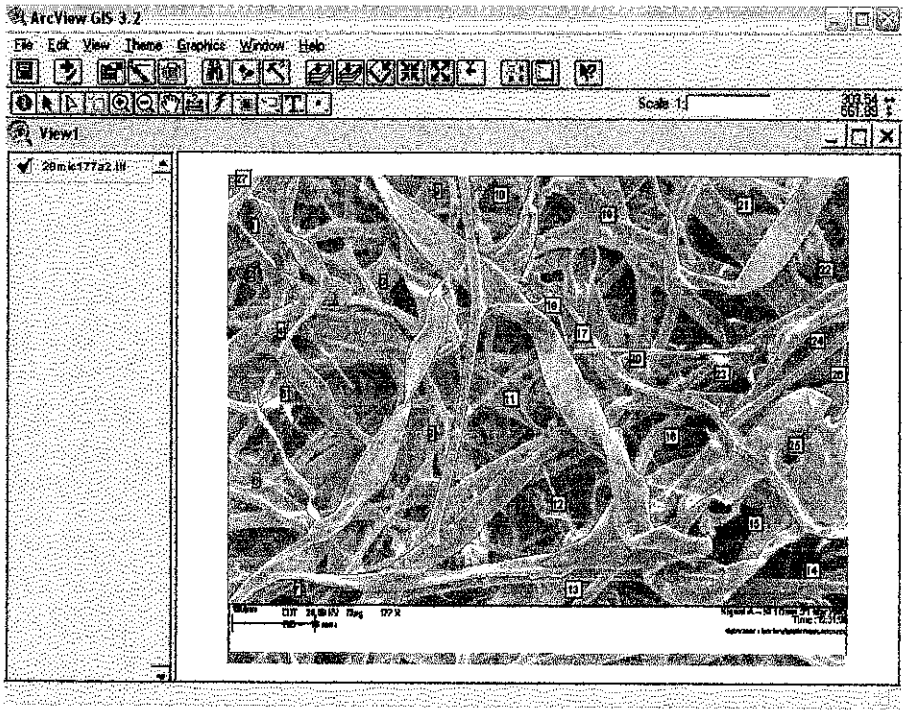

   - Sample B

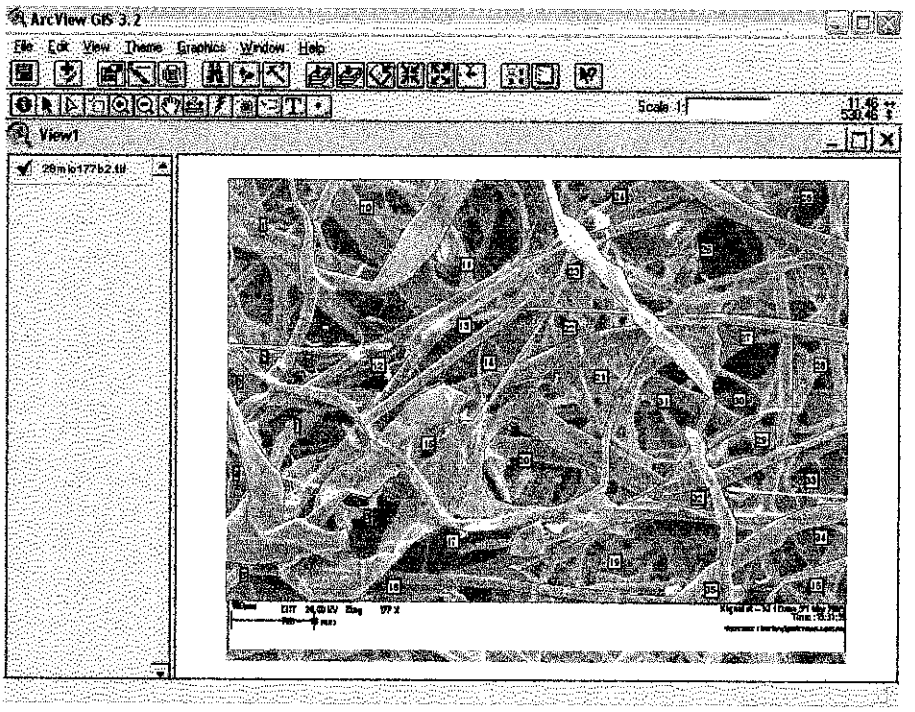

- Sample C

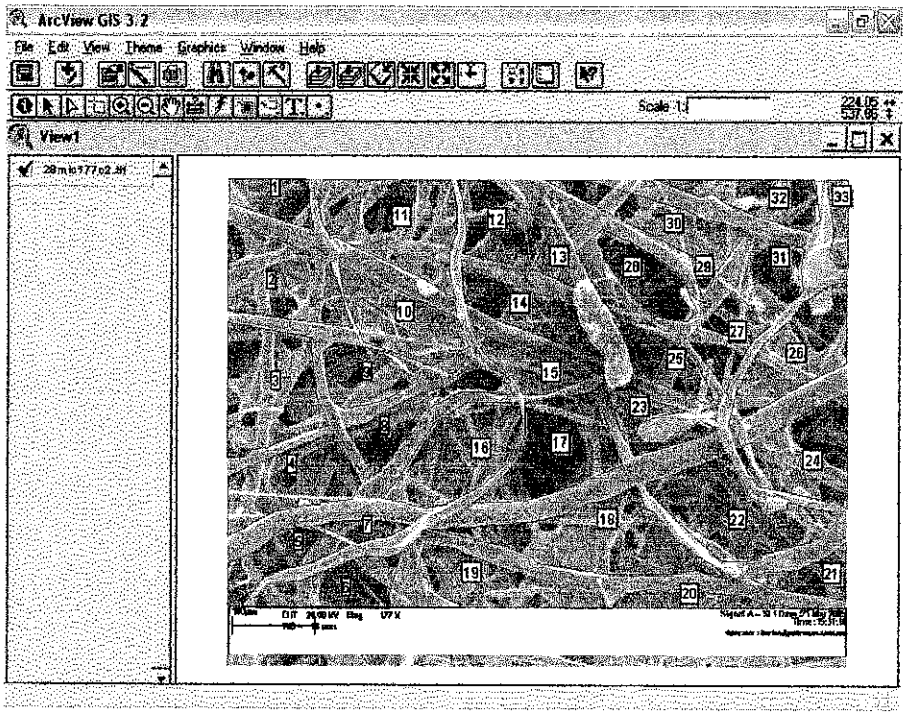

2. 50 micron

- Sample A

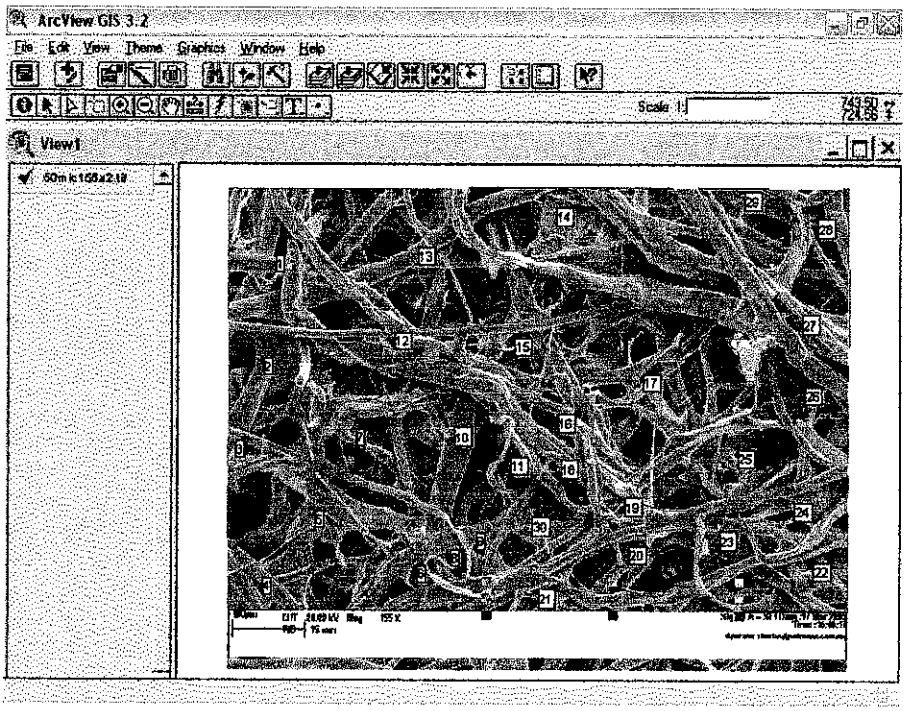

- Sample B

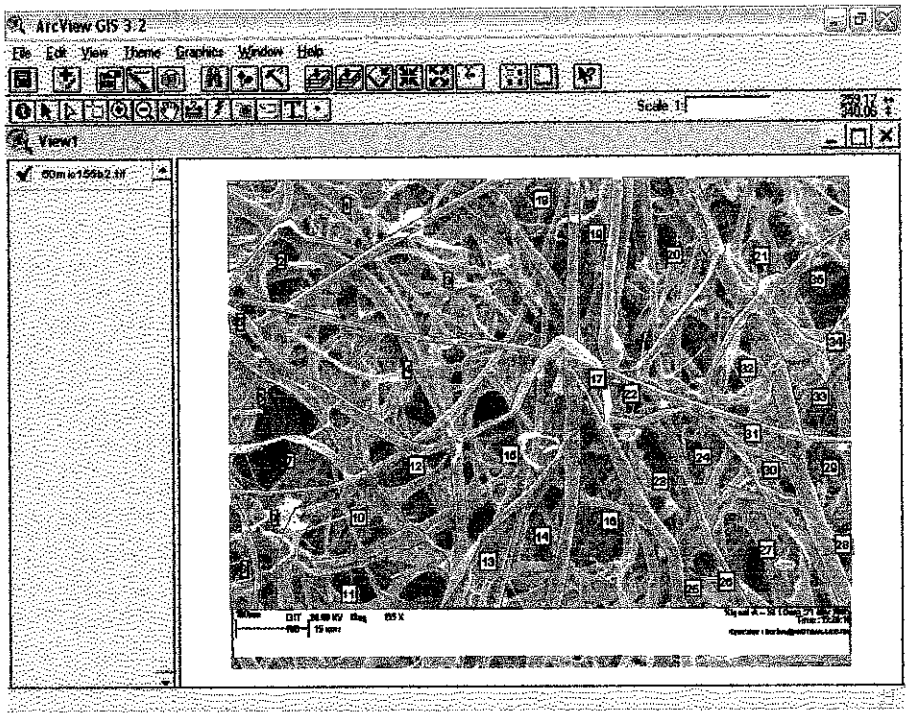

- Sample C

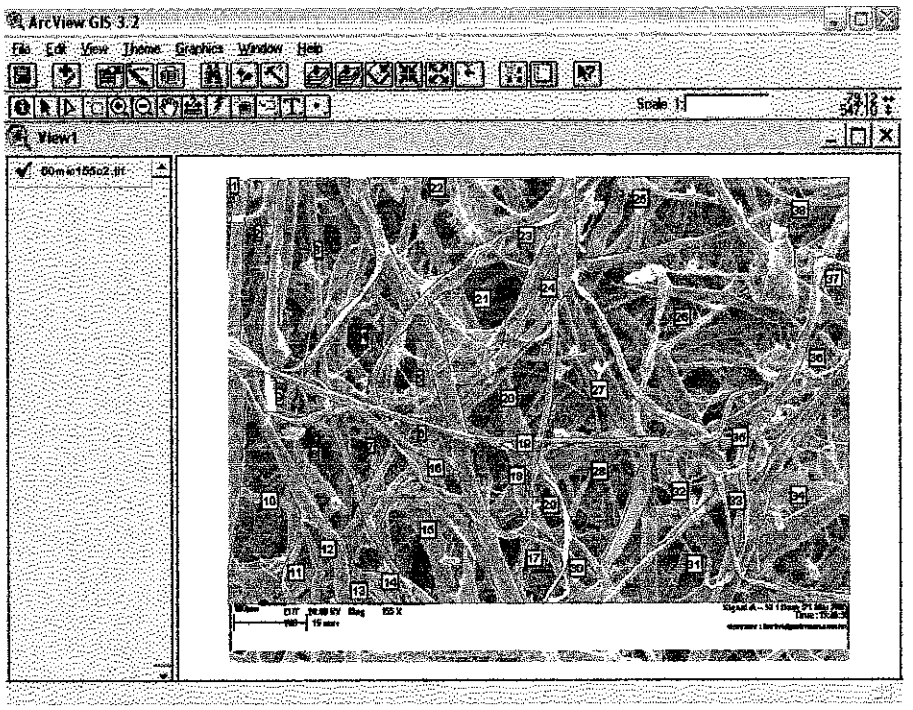

APPENDIX 13: Porosity Calculations

Appendix 13-1: 10 micron

SAMPLE A

Total Area = 690103.7

No	Area
1	29840.05
2	5070.99
3	903.55
4	11134.36
5	11353.92
6	621.69
7	21536
8	36728.63
9	6889.2
10	11001.75
11	5111.7
12	611.21
13	12060.11
14	5301.66
15	5070.38
16	12418.45
17	33346.94
18	41888.44
19	543.98
20	36248.79
21	18615.65
22	2481.22
23	2745.81
24	34909.81
25	12576.96
26	52360.4
27	4681.2
28	41720.07
29	5991.2
30	8594.54
31	1446.92
32	11645.65
Summation	485451.2

Porosity = **0.703447**

= **70.34468 %**

SAMPLE B

Total Area = 690103.7

No	Area
1	5356.82
2	1720.21
3	29922.34
4	4990.71
5	18554.43
6	7423
7	12787.7
8	26113.19
9	16123.01
10	29799.72
11	10564.74
12	9834.27
13	390.64
14	29981.9
15	20650.38
16	20717.83
17	580.7
18	1033.53
19	2603.96
20	40023.75
21	6357.06
22	10610.29
23	8805.12
24	4191.91
25	1179.8
26	2356.97
27	9988.42
28	16385.77
29	1002
30	36260.14
31	756.75
32	2195.85
33	8979.42
34	13554.96
35	7366.94
Summation	419164.2

Porosity = **0.607393**

= **60.73931 %**

SAMPLE C

Total Area = 690103.7

No	Area
1	1253.51
2	5504.6
3	6880.75
4	4619.82
5	7599.89
6	4247.11
7	1484.46
8	9447.5
9	20531.56
10	3005.55
11	4861.12
12	29674.84
13	20015.5
14	45162.11
15	14601.69
16	1656.48
17	13147.49
18	11596.14
19	6336.03
20	5099.24
21	4455.77
22	41831.63
23	19860.21
24	4059.96
25	18583.61
26	11363.59
27	1106.18
28	9667.3
29	20294.24
30	3938.12
31	6681.66
32	3169.61
33	6931.72
34	2888.48
35	16379.22
36	4133.23
37	2338.98
38	4209.68
39	2963.34
40	15497.62
41	4817.32
Summation	421896.9

Porosity = **0.611353**

= **61.13529 %**

Average Porosity = ***64.07 %***

Appendix 13-2: 28 micron

SAMPLE A

Total Area = 690407.9

No	Area
1	4754.48
2	10099.19
3	60616.48
4	407.24
5	20932.41
6	17035.84
7	2709.73
8	36317.91
9	5168.13
10	6932.38
11	32283.22
12	26513.48
13	13525.15
14	16588.72
15	12223.68
16	31146.65
17	858.63
18	174.74
19	47855.26
20	629.37
21	20567.88
22	26864.48
23	11615.67
24	3840.33
25	692.37
26	2950.37
27	22.07
Summation	413325.9

Porosity = **0.598669**

= **59.86691 %**

SAMPLE B

Total Area = 690407.9

No	Area
1	17716.78
2	939.34
3	2464.34
4	2271.11
5	4642.41
6	9216.83
7	22499.94
8	2218.03
9	2268.72
10	21084.67
11	30261.54
12	5040.21
13	4865.46
14	12278.17
15	747.89
16	3570.07
17	8745.07
18	4278.6
19	20672.56
20	15911.46
21	17441.24
22	668.57
23	7654.25
24	10451.38
25	7520.65
26	46828.45
27	6881.32
28	8327.59
29	3120.98
30	5544.77
31	24740.63
32	1583.45
33	13620.67
34	10016.01
35	366.79
Summation	356460

Porosity = **0.516303**

= **51.63034 %**

SAMPLE C

Total Area = 690407.9

No	Area
1	5509.8
2	10402.82
3	12046.12
4	16335.37
5	8815.9
6	11830.41
7	2779.29
8	10640.21
9	11148.59
10	12758.28
11	25333.38
12	10103.65
13	1688.82
14	10779.56
15	6573.17
16	21248.99
17	22450.03
18	28428.1
19	14260.66
20	3721.26
21	6600.27
22	26430.35
23	5743.94
24	15635.13
25	8575.26
26	18291.93
27	7658.22
28	14813.48
29	639.54
30	13776.13
31	5878.35
32	7331.95
33	3454.6
Summation	381683.6

Porosity = **0.552838**

= **55.28377 %**

Average Porosity = ***55.59 %***

Appendix 13-3: 50 micron

SAMPLE A

Total Area = 690976.9

No	Area
1	23990.52
2	10457.53
3	1237.58
4	1194.83
5	51182.13
6	2614.85
7	8922.12
8	2141.2
9	1238.18
10	42945.83
11	2755.36
12	1631.25
13	60415.98
14	46942.54
15	7856.64
16	5904.34
17	56729.14
18	1503.77
19	1713.14
20	16218.56
21	4657.65
22	18384.88
23	2928.44
24	10168.12
25	31553.1
26	10292.82
27	3211.33
28	15515.07
29	12362.36
30	12136.24
Summation	468805.5

Porosity = 0.678468

= 67.84677 %

SAMPLE B

Total Area = 690976.9

No	Area
1	17222.9
2	10381.06
3	54680.93
4	51122.67
5	1215.32
6	9964.1
7	10031.11
8	3273.66
9	9503.29
10	11736.19
11	16284.73
12	18352.17
13	6823.64
14	7669.15
15	23950.57
16	30823.84
17	1346.03
18	1911.91
19	9462.75
20	30533.46
21	36045.81
22	3979.35
23	14893.2
24	10168.44
25	597.32
26	461.64
27	25023.59
28	512.93
29	3926.4
30	2471.17
31	1330.31
32	10309.09
33	9903.7
34	1039.1
35	10856.76
Summation	457808.3

Porosity = 0.662552

= 66.25523 %

SAMPLE C

Total Area = 690976.9

No	Area
1	215.62
2	9191.01
3	29283.87
4	12243.86
5	9937.78
6	2865.53
7	8604.92
8	15237.6
9	5551.24
10	22477.19
11	2660.73
12	2226.99
13	904.12
14	1582.62
15	24775.78
16	2509.21
17	6556.09
18	9569.81
19	527.82
20	15825.36
21	17227.32
22	34140.79
23	3390.02
24	1789.92
25	20337.58
26	66971.19
27	26063.69
28	17277.28
29	4162.6
30	3463.28
31	18274.63
32	14721.44
33	2480.08
34	32097.79
35	3149.42
36	11665.26
37	1958.92
38	6308.83
Summation	468227.2

Porosity = 0.677631

= 67.76308 %

Average Porosity = ***67.29 %***

APPENDIX 14: Permeability Calculations

Appendix 14-1: 10 Micron

Table 1: Sample A

Compressor frequency, Hz	ΔP Across Filter Media, in H_2O	Downstream Velocity, m/s
3.50	0.2	0.08
4.00	0.6	0.13
4.50	0.8	0.18
5.00	1.1	0.20
5.50	1.3	0.22
6.00	1.5	0.27
6.50	1.8	0.32

Table 2: Sample B

Compressor frequency, Hz	ΔP Across Filter Media, in H_2O	Downstream Velocity, m/s
3.50	0.3	0.07
4.00	0.6	0.11
4.50	0.8	0.16
5.00	1.0	0.21
5.50	1.2	0.23
6.00	1.5	0.25
6.50	1.8	0.30

Table 3:Sample C

Compressor frequency, Hz	ΔP Across Filter Media, in H_2O	Downstream Velocity, m/s
3.50	0.5	0.08
4.00	0.7	0.11
4.50	0.9	0.14
5.00	1.0	0.20
5.50	1.3	0.22
6.00	1.5	0.25
6.50	1.8	0.30

Table 4: Average

Compressor frequency, Hz	ΔP Across Filter Media, in H_2O	ΔP Across Filter Media, in Pa	Downstream Velocity, m/s	P, Pa	$\boxed{\Delta P \bullet P}$, Pa	Reynolds Number for Downstream Filter Media	Flow average pore diameter, d	Permeability Coefficient, K_v	Viscous Term Coefficient, α
3.50	0.333	83.0	0.077	101341.5	8411344.500	149.954	2.39108E-05	7.33414E-12	136348654390.690
4.00	0.633	157.7	0.117	101378.9	15987444.645	228.191	2.13948E-05	5.87186E-12	170303777520.949
4.50	0.833	207.5	0.160	101403.8	21041278.125	312.948	2.18398E-05	6.11865E-12	163434655266.993
5.00	1.033	257.3	0.203	101428.7	26097591.645	397.705	2.21069E-05	6.26926E-12	159508513620.746
5.50	1.267	315.4	0.223	101457.7	31999758.580	436.823	2.09232E-05	5.61584E-12	178067708888.690
6.00	1.500	373.5	0.257	101486.8	37905301.125	502.021	2.06091E-05	5.44851E-12	183536522024.814
6.50	1.800	448.2	0.307	101524.1	45503101.620	599.817	2.05607E-05	5.42292E-12	184402347225.518

Experimental Conditions:

1. Air at compressor inlet and downstream of filter paper under test are at ambient conditions, i.e. at T = 22.2 °C and P = 101300 Pa
2. Diameter of pipe, d = 3 cm = 0.03 m
3. Thickness of the medium, z = 0.0004333 m
4. Porosity taken from SEM calculation, ε = 0.6407

At atm pressure and T = 22.2 °C,

ρ = 1.1952 kg/m³
μ = 0.000018332 Pa.s
P = 101300 Pa

Tabulating the data into Graph

Log $\Delta P \bullet P$	Log u_2
6.9249	-1.1154
7.2038	-0.8331
7.3231	-0.7959
7.4166	-0.6918
7.5051	-0.6510
7.5787	-0.5906
7.6580	-0.5133

Estimating the flow average pore diameter, d

The flow average pore diameter is given by the equation:

$$\mathbf{d}^2 = \frac{32\, u_2 \mu z P_2}{\varepsilon^2 \Delta P \mathbf{P}} \quad = \quad \mathbf{d}^2 = \frac{32B}{\varepsilon^2}$$

Thus,

$$K_v = \frac{u_2 \mu z P_2}{\Delta P \mathbf{P}}$$

Average Permeability Coefficient, $K_{v,ave}$ = 5.79117E-12 m^2

Flow average pore diameter, d_p = 2.16206E-05 m
= 21.62 micron

Permeability value can be obtain using the equation below:

$$\frac{Q}{A\ \Delta\ P} = \frac{K_v}{\mu\ z}$$ in the units of $\frac{m^3/s}{m^2 Pa}$

Hence:

Permeability = 0.000729068 $\frac{m^3/s}{m^2 Pa}$

Also,

$$K_v = \frac{\mathbf{d}^2 \varepsilon}{32\ \tau} = \frac{\mathbf{d}^2 \varepsilon^2}{32} = \frac{d^2 \varepsilon}{16\ k}$$ and $$d = \frac{d_f \varepsilon}{1-\varepsilon}$$

Referring to Figure 5;

With the porosity value from SEM experiment, the value k can be interpolated to 6.4221

Specific pore diameter, d = 3.04758E-05 m = 30.48 micron

From;

$$d = \frac{d_f \varepsilon}{1-\varepsilon}$$

Fiber diameter, d_f = 1.70906E-05 = 17.09 micron

Average viscous-term coefficient, α_{ave} = 1679431684419.771 m^{-2}

Appendix 14-2: 28 Micron

Table 1: Sample A

Compressor frequency, Hz	ΔP Across Filter Media, in H_2O	Downstream Velocity, m/s
3.50	0.2	0.14
4.00	0.4	0.15
4.50	0.7	0.20
5.00	0.8	0.29
5.50	1.1	0.31
6.00	1.3	0.34
6.50	1.5	0.37

Table 2: Sample B

Compressor frequency, Hz	ΔP Across Filter Media, in H_2O	Downstream Velocity, m/s
3.50	0.3	0.10
4.00	0.5	0.14
4.50	0.7	0.18
5.00	0.9	0.25
5.50	1.1	0.30
6.00	1.3	0.34
6.50	1.5	0.40

Table 3:Sample C

Compressor frequency, Hz	ΔP Across Filter Media, in H_2O	Downstream Velocity, m/s
3.50	0.3	0.12
4.00	0.5	0.17
4.50	0.7	0.21
5.00	0.9	0.26
5.50	1.1	0.30
6.00	1.3	0.32
6.50	1.5	0.38

Table 4: Average

Compressor frequency, Hz	ΔP Across Filter Media, in H_2O	ΔP Across Filter Media, in Pa	Downstream Velocity, m/s	P, Pa	$\boxed{\Delta P \bullet P}$, Pa	Reynolds Number for Downstream Filter Media	Flow average pore diameter, d	Permeability Coefficient, K_v	Viscous Term Coefficient, α
3.50	0.267	66.4	0.120	101333.2	6728524.480	234.711	4.6604E-05	2.09744E-11	47677097541.234
4.00	0.467	116.2	0.153	101358.1	11777811.220	299.908	3.98179E-05	1.53108E-11	65312939473.233
4.50	0.700	174.3	0.197	101387.2	17671780.245	384.665	3.68144E-05	1.30882E-11	76404821141.139
5.00	0.867	215.8	0.267	101407.9	21883824.820	521.580	3.85226E-05	1.43309E-11	69779156504.353
5.50	1.100	273.9	0.303	101437.0	27783580.605	593.297	3.64635E-05	1.28399E-11	77882394431.304
6.00	1.300	323.7	0.333	101461.9	32843200.845	651.975	3.51568E-05	1.19361E-11	83779535642.148
6.50	1.500	373.5	0.383	101486.8	37905301.125	749.771	3.50939E-05	1.18934E-11	84080364062.476

Experimental Conditions:

1. Air at compressor inlet and downstream of filter paper under test are at ambient conditions, i.e. at T = 22.2 °C and P = 101300 Pa
2. Diameter of pipe, d = 3 cm = 0.03 m
3. Thickness of the medium, z = 0.0006333 m
4. Porosity taken from SEM calculation, ε = 0.5559

At atm pressure and T = 22.2 °C,

ρ = 1.1952 kg/m^3

μ = 0.000018332 Pa.s

P = 101300 Pa

Tabulating the data into Graph

Log $\Delta P \bullet \mathbf{P}$	Log u_2
6.8279	-0.9208
7.0711	-0.8144
7.2473	-0.7063
7.3401	-0.5740
7.4438	-0.5181
7.5164	-0.4771
7.5787	-0.4164

Estimating the flow average pore diameter, d

The flow average pore diameter is given by the equation:

$$\mathbf{d}^2 = \frac{32\, u_2 \mu z P_2}{\varepsilon^2 \Delta P \mathbf{P}} = \mathbf{d}^2 = \frac{32B}{\varepsilon^2}$$

Thus,

$$K_v = \frac{u_2 \mu z P_2}{\Delta P \mathbf{P}}$$

Average Permeability Coefficient, $K_{v,ave}$ = 1.43391E-11 m^2

Flow average pore diameter, d_p = 3.88965E-06 m
= 33.75 micron

Permeability value can be obtain using the equation below:

$$\frac{Q}{A\ \Delta\ P} = \frac{K_v}{\mu\ z}$$ in the units of $\frac{m^3/s}{m^2 Pa}$

Hence:

Permeability = 0.001235102 $\frac{m^3/s}{m^2 \cdot Pa}$

Also,

$$K_v = \frac{\mathbf{d}^2 \varepsilon}{32\ \tau} = \frac{\mathbf{d}^2 \varepsilon^2}{32} = \frac{d^2 \varepsilon}{16\ k}$$ and $$d = \frac{d_f \varepsilon}{1-\varepsilon}$$

Referring to Figure 5;

With the porosity value from SEM experiment, the value k can be interpolated to 6.0795

Specific pore diameter, d = 5.00907E-05 m = 50.09 micron

From;

$$d = \frac{d_f \varepsilon}{1-\varepsilon}$$

Fiber diameter, d_f = 4.00167E-05 = 40.02 micron

Average viscous-term coefficient, α_{ave} = 70139324122.235 m^{-2}

Appendix 14-3: 50 Micron

Table 1: Sample A

Compressor frequency, Hz	ΔP Across Filter Media, in H_2O	Downstream Velocity, m/s
3.50	0.2	0.14
4.00	0.5	0.19
4.50	0.7	0.25
5.00	0.9	0.31
5.50	1.1	0.33
6.00	1.3	0.37
6.50	1.5	0.44

Table 2: Sample B

Compressor frequency, Hz	ΔP Across Filter Media, in H_2O	Downstream Velocity, m/s
3.50	0.3	0.14
4.00	0.6	0.18
4.50	0.7	0.25
5.00	0.9	0.31
5.50	1.1	0.33
6.00	1.3	0.38
6.50	1.6	0.43

Table 3:Sample C

Compressor frequency, Hz	ΔP Across Filter Media, in H_2O	Downstream Velocity, m/s
3.50	0.3	0.13
4.00	0.5	0.17
4.50	0.7	0.23
5.00	0.8	0.29
5.50	1.1	0.33
6.00	1.3	0.38
6.50	1.6	0.48

Table 4: Average

Compressor frequency, Hz	ΔP Across Filter Media, in H_2O	ΔP Across Filter Media, in Pa	Downstream Velocity, m/s	P, Pa	$\Delta P \bullet P$, Pa	Reynolds Number for Downstream Filter Media	Flow average pore diameter, d	Permeability Coefficient, K_v	Viscous Term Coefficient, α
3.50	0.267	66.4	0.137	101333.2	6728524.480	267.310	4.26787E-05	2.57735E-11	38799534947.800
4.00	0.533	132.8	0.180	101366.4	13461457.920	352.066	3.46282E-05	1.69672E-11	58937115689.421
4.50	0.700	174.3	0.243	101387.2	17671780.245	475.942	3.51399E-05	1.74724E-11	57233193877.663
5.00	0.867	215.8	0.303	101407.9	21883824.820	593.297	3.52564E-05	1.75885E-11	56855486144.913
5.50	1.100	273.9	0.330	101437.0	27783580.605	645.455	3.26364E-05	1.50715E-11	66350402248.659
6.00	1.300	323.7	0.377	101461.9	32843200.845	736.731	3.20698E-05	1.45527E-11	68715952803.447
6.50	1.567	390.1	0.450	101495.1	39593219.005	880.166	3.19254E-05	1.44219E-11	69339001551.899

Experimental Conditions:

1. Air at compressor inlet and downstream of filter paper under test are at ambient conditions, i.e. at T = 22.2 °C and P = 101300 Pa
2. Diameter of pipe, d = 3 cm = 0.03 m
3. Thickness of the medium, z = 0.0006833 m
4. Porosity taken from SEM calculation, ε = 0.6729

At atm pressure and T = 22.2 °C,

ρ = 1.1952 kg/m^3

μ = 0.000018332 Pa.s

P = 101300 Pa

Tabulating the data into Graph

Log $\Delta P \bullet P$	Log u_2
6.8279	-0.8643
7.1291	-0.7447
7.2473	-0.6138
7.3401	-0.5181
7.4438	-0.4815
7.5164	-0.4240
7.5976	-0.3468

Estimating the flow average pore diameter, d

The flow average pore diameter is given by the equation:

$$\mathbf{d}^2 = \frac{32\, u_2 \mu z P_2}{\varepsilon^2 \Delta P \mathbf{P}} = \mathbf{d}^2 = \frac{32B}{\varepsilon^2}$$

Thus,

$$K_v = \frac{u_2 \mu z P_2}{\Delta P \mathbf{P}}$$

Average Permeability Coefficient, $K_{v,ave}$ = 1.74068E-11 m^2

Flow average pore diameter, d_p = 3.54018E-05 m
= 37.18 micron

Permeability value can be obtain using the equation below:

$$\frac{Q}{A\ \Delta\ P} = \frac{K_v}{\mu\ z}$$ in the units of $\frac{m^3/s}{m^2 Pa}$

Hence:

Permeability = 0.001389626 $\frac{m^3/s}{m^2 Pa}$

Also,

$$K_v = \frac{\mathbf{d}^2 \varepsilon}{32\ \tau} = \frac{\mathbf{d}^2 \varepsilon^2}{32} = \frac{d^2 \varepsilon}{16\ k}$$ and $$d = \frac{d_f \varepsilon}{1-\varepsilon}$$

Referring to Figure 5;

With the porosity value from SEM experiment, the value k can be interpolated to **6.5187**

Specific pore diameter, d = 5.19427E-05 m = **51.94 micron**

From;

$$d = \frac{d_f \varepsilon}{1-\varepsilon}$$

Fiber diameter, d_f = 2.52496E-05 = **25.25 micron**

Average viscous-term coefficient, α_{ave} = **57315280951.934 m^{-2}**